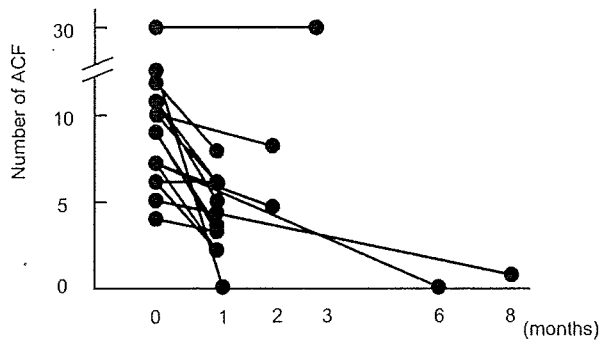

Fig. 1. The numbers of ACF were prospectively examined in 14 subjects before and after 1 – 8 months of pioglitazone treatment. After PPARγ ligand treatment, the number of ACF significantly decreased.

agents in average-risk individuals.

ACF and PPARγ

PPARγ is mainly expressed in adipose tissue and plays a central role in adipocyte differentiation and insulin sensitivity. Activating synthetic ligands for PPARγ, such as pioglitazone, are commonly used to treat diabetes. PPARγ is also overexpressed in many tumors. This suggests that modulation of PPARγ expression or function might have impact on tumor cell survival. Chemopreventive effects of PPARγ ligand on the formation of the human ACF were evaluated. Fourteen patients were examined for ACF by magnifying colonoscopy before and after 1 to 8 months of pioglitazone treatment (Fig. 1). After PPARγ ligand treatment, the number of ACF was significantly decreased. These results suggest that a PPARγ ligand is a promising candidate as a chemopreventive agent for CRC.

Conclusions

Our results suggest that visceral fat obesity may be a risk factor for CRC and visceral fat may play an important role in colorectal carcinogenesis at an earlier stage in the adenoma-carcinoma sequence (25). Adipocytokines secreted by visceral fat tissue and/or the visceral fat itself may play an important role in colon carcinogenesis. PPARγ ligand is a promising candidate for CRC chemoprevention.

Acknowledgments

We thank Masako Ochiai and Machiko Hiraga for their technical assistance. This work was supported in part by a Grant-in-Aid for research on the Third Term Comprehensive Control Research for Cancer from the Ministry of Hearth, Labour, and Welfare, Japan to A.N.; a grant from the National Institute of Biomedical Innovation (NBIO) to A.N.; a grant from the Ministry of Education, Culture, Sports, Science, and Technology, Japan (KIBAN-B) to A.N.; a grant from the Ministry of Education, Culture, Sports, Science, and Technology, Japan (WAKATE-B) to H.T.; a research grant of the Princess Takamatsu Cancer Research Fund to A.N.; and a grant for 2007 Strategic Research Project (No. K19041) of Yokohama City University, Japan to H.T. and A.N.

References

1 Fujioka S, Matsuzawa Y, Tokunaga K, Tarui S. Contribution of intra-abdominal fat accumulation to the impairment of glucose and lipid metabolism in human obesity. Metabolism. 1987;36: 54–59.
2 Larsson B, Svardsudd K, Welin L, Wilhelmsen L, Björntorp P, Tibblin G. Abdominal adipose tissue distribution, obesity, and risk of cardiovascular disease and death: 13 year follow up of participants in the study of men born in 1913. Br Med J. 1984;288:1401–1404.
3 Kissebah AH, Vydelingum N, Murray R, Evans DJ, Hartz AJ, Kalkhoff RK, et al. Relation of body fat distribution to metabolic complications of obesity. J Clin Endocrinol Metab. 1982;54: 254–260.
4 Folsom AR, Kaye SA, Sellers TA, Hong CP, Cerhan JR, Potter JD, et al. Body fat distribution and 5-year risk of death in older women. JAMA. 1993;269:483–487.
5 Anderson WF, Umar A, Brawley OW. Colorectal carcinoma in black and white race. Cancer Metastasis Rev. 2003;22:67–82.
6 Rougier P, Mitry E. Epidemiology, treatment and chemoprevention in colorectal cancer. Ann Oncol. 2003;14:ii3–ii5.
7 Kinzler KW, Vogelstein B, Lessons from hereditary colorectal cancer. Cell. 1996;87:159–170.
8 Fearon ER, Vogelstein B. A genetic model for colorectal tumorigenesis. Cell. 1990;61:759–767.
9 Limburg PJ, Anderson KE, Johnson TW, Jacobs DR, Lazovich D, Hong CP, et al. Diabetes mellitus and subsite-specific colorectal cancer risks in the Iowa Women's Health Study. Cancer Epidemiol Biomarkers Prev. 2005;14:133–137.
10 Chang CK, Ulrich CM. Hyperinsulinaemia and hyperglycaemia: possible risk factors of colorectal cancer among diabetic patients. Diabetologia. 2003;46:595–607.
11 Larsson SC, Giovannucci E, Wolk A. Diabetes and colorectal cancer incidence in the cohort of Swedish men. Diabetes Care. 2005;28:1805–1809.
12 Hu FB, Manson JE, Liu S, Hunter D, Colditz GA, Michels KB, et al. Prospective study of adult onset diabetes mellitus (type 2) and risk of colorectal cancer in women. J Natl Cancer Inst. 1999;91:542–547.
13 Schoen RE, Tangen CM, Kuller LH, Burke GL, Cushman M, Tracy RP, et al. Increased blood glucose and insulin, body size, and indent colorectal cancer. J Natl Cancer Inst. 1999;91:1147–1154.
14 Giovannucci E, Aasherio A, Rimm EB, Colditz GA, Stampfer

MJ, Willett WC. Physical activity, obesity, and risk for colon cancer and adenoma in men. Ann Intern Med. 1995;122:327–334.

15 Frezza EE, Wachtel MS, Chiriva-Internati M. Influence of obesity on the risk of developing colon cancer. Gut. 2006;55: 285–291.

16 Slattery ML, Ballard-Barbash R, Edwards S, Caan BJ, Potter JD. Body mass index and colon cancer: an evaluation of the modifying effects of estrogen (United States). Cancer Causes Control. 2003;14:75–84.

17 Giovannucci E. Diet, body weight, and colorectal cancer: a summary of the epidemiologic evidence. J Womens Health. 2003;12:173–182.

18 El-Serag HB. Obesity and disease of the oesophagus and colon. Gastroenterol Clin North Am. 2005;34:63–82.

19 World Health Organization. Definition, diagnosis, and classification of diabetes mellitus and its complications: report of a WHO consultation. Geneva: World Health Organization; 1999.

20 Bird RP. Observation and quantification of aberrant crypts in the murine colon treated with a colon carcinogen: preliminary findings. Cancer Lett. 1987;37:147–151.

21 Pretlow TP, O'Riordan MA, Somich GA, Amini SB, Pretlow TG. Aberrant crypts correlate with tumor incidence in F344 rats treated with azoxymethane and phytate. Carcinogenesis. 1992;13:1509–1512.

22 Takayama T, Katsuki S, Takahashi Y, Ohi M, Nojiri S, Sakamaki S, et al. Aberrant crypt foci of the colon as precursors of adenoma and cancer. N Engl J Med. 1998;339:1277–1284.

23 Sutherland LA, Bird RP. The effect of chenodeoxycholic acid on the development of aberrant crypt foci in the rat colon. Cancer Lett. 1994;76:101–107.

24 Roncucci L, Stamp D, Medline A, Cullen JB, Bruce WR. Identification and quantification of aberrant crypt foci and microadenomas in the human colon. Hum Pathol. 1991;22:287–294.

25 Pretlow TP, Barrow BJ, Ashton WS, O'Riordan MA, Pretlow TG, Jurcisek JA, et al. Aberrant crypts: putative preneoplastic foci in human colonic mucosa. Cancer Res. 1991;51:1564–1567.

The American Journal of Pathology, Vol. 171, No. 6, December 2007
Copyright © American Society for Investigative Pathology
DOI: 10.2353/ajpath.2007.070741

Molecular Pathogenesis of Genetic and Inherited Diseases

Chronic Oxidative Stress Causes Amplification and Overexpression of *ptprz1* Protein Tyrosine Phosphatase to Activate β-Catenin Pathway

Yu-Ting Liu,* Donghao Shang,† Shinya Akatsuka,* Hiroki Ohara,* Khokon Kumar Dutta,* Katsura Mizushima,‡ Yuji Naito,‡ Toshikazu Yoshikawa,§ Masashi Izumiya,¶ Kouichiro Abe,¶ Hitoshi Nakagama,¶ Noriko Noguchi,‖ and Shinya Toyokuni*

From the Departments of Pathology and Biology of Diseases and Urology,† Graduate School of Medicine, Kyoto University, Kyoto; Medical Proteomics,‡ and Inflammation and Immunology,§ Graduate School of Medicine, Kyoto Prefectural University of Medicine, Kyoto; the Biochemistry Division,¶ National Cancer Center Research Institute, Tokyo; and the Science and Engineering Research Institute,‖ Doshisha University, Kyoto, Japan*

Ferric nitrilotriacetate induces oxidative renal tubular damage via Fenton-reaction, which subsequently leads to renal cell carcinoma (RCC) in rodents. Here, we used gene expression microarray and array-based comparative genomic hybridization analyses to find target oncogenes in this model. At the common chromosomal region of amplification (4q22) in rat RCCs, we found *ptprz1*, a tyrosine phosphatase (also known as protein tyrosine phosphatase ζ or receptor tyrosine phosphatase β) highly expressed in the RCCs. Analyses revealed genomic amplification up to eightfold. Despite scarcity in the control kidney, the amounts of PTPRZ1 were increased in the kidney after 3 weeks of oxidative stress, and mRNA levels were increased 16~552-fold in the RCCs. Network analysis of the expression revealed the involvement of the β-catenin pathway in the RCCs. In the RCCs, dephosphorylated β-catenin was translocated to nuclei, resulting in the expression of its target genes *cyclin D1*, *c-myc*, c-jun, fra-1, and *CD44*. Furthermore, knockdown of *ptprz1* with small interfering RNA (siRNA), in FRCC-001 and FRCC-562 cell lines established from the induced RCCs, decreased the amounts of nuclear β-catenin and suppressed cellular proliferation concomitant with a decrease in the expression of target genes. These results demonstrate that chronic oxidative stress can induce genomic amplification of *ptprz1*, activating β-catenin pathways without the involvement of Wnt signaling for carcinogenesis. Thus, iron-mediated persistent oxidative stress confers an environment for gene amplification. *(Am J Pathol 2007, 171:1978–1988; DOI: 10.2353/ajpath.2007.070741)*

Oxidative stress is associated with a plethora of pathological conditions, including infection, inflammation, UV and γ-irradiation, and overload of transition metals and certain chemical compounds.[1] Many epidemiological studies demonstrated a close association between chronically oxidative conditions and carcinogenesis. Chronic tuberculous pleuritis causes a high incidence of malignant lymphoma[2]; chronic *Helicobacter pylori* infection is associated with a high incidence of gastric cancer[3]; inflammatory bowel diseases are risk factors for colorectal cancer[4]; a high risk for heptocellular carcinoma is found in patients with genetic hemochromatosis[5,6]; exposure to asbestos fibers rich in iron is frequently associated with mesothelioma and lung cancer[7]; severe burn by UV radiation is a risk factor for skin cancer[8]; and γ-irradiation causes a high incidence of leukemia.[9] As an initiation process under these circumstances and also as a coordinated strategy in proliferating tumor cells,[10] oxidative stress appears to play a role in human carcinogenesis. Thus, an analysis that determines genomic and expressional alterations in an established oxidative stress-induced carcinogenesis is of great importance.

Supported in part by a Grant-in-Aid from the Ministry of Education, Culture, Sports, Science and Technology of Japan, a MEXT grant (Special Coordination Funds for Promoting Science and Technology), a grant of Long-range Research Initiative by Japan Chemical Industry Association, and a Grant-in-Aid for Cancer Research from the Ministry of Health, Labour and Welfare of Japan.

Accepted for publication September 6, 2007.

Address reprint requests to Shinya Toyokuni, M.D., Ph.D., Department of Pathology and Biology of Diseases, Graduate School of Medicine, Kyoto University, Kyoto, Japan. E-mail: toyokuni@path1.med.kyoto-u.ac.jp.

An iron chelate, ferric nitrilotriacetate (Fe-NTA) causes oxidative renal proximal tubular damage via a Fenton reaction that ultimately leads to a high incidence of renal cell carcinoma (RCC) in mice[11] and rats[12] after repeated intraperitoneal administration. This model is intriguing in that 1) more than half of the induced tumors metastasize to the lung and/or invade the peritoneal cavity, resulting in animal mortality[13]; 2) evidence exists for the involvement of free radical reactions in carcinogenesis, including not only covalently modified macromolecules (oxidatively modified DNA bases[14,15] and lipid peroxidation products[16,17]) but also preventive action of α-tocopherol against carcinogenesis[18]; and 3) genetic changes in $p16^{INK4a}$ tumor suppressor gene, especially large deletions,[19,20] and expressional alteration of several key genes, including *annexin 2* overexpression[21] and also loss of *thioredixn-binding protein-2* based on methylation of the promoter region,[22] have been observed.

Here, we performed array-based comprehensive genomic hybridization and gene expression microarray analyses using Fe-NTA-induced rat RCCs and their cell lines to find amplified oncogenes in this model. A common chromosomal amplification at 4q22 in cancers resulted in the discovery of β-catenin pathway activation via gene amplification and overexpression of *ptprz1* protein tyrosine phosphatase.

Materials and Methods

Animal Experiments and Chemicals

The carcinogenesis study was performed as previously described[13] using specific pathogen-free male Wistar rats (Shizuoka Laboratory Animal Center, Shizuoka, Japan) or male F1 rats hybrid between Fischer344 and Brown-Norway strains (Charles River, Yokohama, Japan). The animals were kept under close observation and were sacrificed when they showed persistent weight loss and distress. Histological grade of tumor was determined according to the modified World Health Organization classification as we previously described.[13] The animal experiment committee of Graduate School of Medicine, Kyoto University approved this experiment. All of the chemicals used were of analytical quality.

Array-Based Comparative Genomic Hybridization

We performed array-based comparative genomic hybridization (CGH) with an Agilent 185K rat genome CGH microarray chip (Agilent Technologies, Santa Clara, CA), as described in the Agilent Oligonucleotide Array-based CGH for Genomic DNA Analysis Protocol ver. 4.0, and analyzed results with CGH Analytics Software (ver. 3.4). For each array, normal kidney tissue was used as a reference and labeled with Cy-3. Samples of interest were each labeled with Cy-5.

Ptprz1 Genome Copy Analysis

Genomic DNA was extracted with a DNA Extractor WB kit (Wako, Osaka, Japan). A Platinum SYBR Green qPCR SuperMix UDG kit (Invitrogen, Carlsbad, CA) and Real-time PCR system 7300 (Applied Biosystems, Foster City, CA) were used. Primer sequences were as follows, based on NW_047689: forward, 5′-CCTTACAGGTGAAAGTCAGC-3′; and reverse, 5′-GGTATACTTTGGCCCACAGT-3′ (130-bp product).

Ptprz1 Genome DNA Fluorescent in Situ Hybridization

Three bacterial artificial chromosome clones (CH230–385 M3, CH 230–160 P8, CH 230–418 P21) were extracted with a big bacterial artificial chromosome DNA isolation kit (Princeton Separations, Adelphia, NJ), labeled with biotin-16-dUTP via nick translation (Roche, Tokyo, Japan) and used as probes (2 μg/ml) for hybridization in ULTRAhyb hybridization buffer (Ambion, Austin, TX) as previously described.[20] Either formalin-fixed paraffin-embedded sections or cell lines were used on MAS-GP-coated glass slides (Matunami Glass Ind., Ltd., Kishiwada, Japan) after smear preparation.

Gene Expression Microarray

A total of 10 microarrays (Rat Genome 230 2.0; 31,999 genes; Affymetrix Inc., Santa Clara, CA) were used for screening purpose: two for each group of untreated control, Fe-NTA treatment for 1 week, Fe-NTA treatment for 3 weeks, Fe-NTA-induced RCCs with neither peritoneal invasion nor metastasis, and Fe-NTA-induced RCCs with pulmonary metastasis. Total RNA was isolated with Isogen (Nippon Gene Co. Ltd., Tokyo, Japan), and the degree of gene expression was then evaluated with GeneChip analysis (Focus array; Affymetrix) as previously described.[23] Network analysis was performed using Ingenuity Pathways Analysis (Ingenuity Systems, Redwood City, CA).

RT-PCR

Total RNA was extracted with TRIzol (Invitrogen), and cDNA was synthesized using RNA PCR kit ver. 3.0 (Takara, Shiga, Japan) with random primers. We then amplified specific cDNA regions for each *ptprz1* isoform with PCR based on a previous report[24] and NM_013080. Primer sequences were as follows: primer set 1 for A, B, and S forms: forward, 5′-atgcgaatcctgcagagcttcc-3′, and reverse, 5′-ggtcagcagacacctctttgtac-3′ (1723-bp product); primer set 2 for A and S forms: forward, 5′-ggcctcgggttgtttatgaca-3′, and reverse, 5′-tgtgtccgaagcagcatgaa-3′ (1700-bp product); primer set 3 for A form: forward, 5′-tcagagcctgcgctctctgaca-3′, and reverse, 5′-gtcaacagtgcagctctgcact-3′ (1745-bp product); and primer set 4 for A and B forms: forward, 5′-ttaggtattacagcagacagctcc-3′, and reverse, 5′-tcagactaaagactccaggctttc-3′ (1737-bp product). For quantitative real-time PCR, a Platinum SYBR Green qPCR SuperMix UDG kit

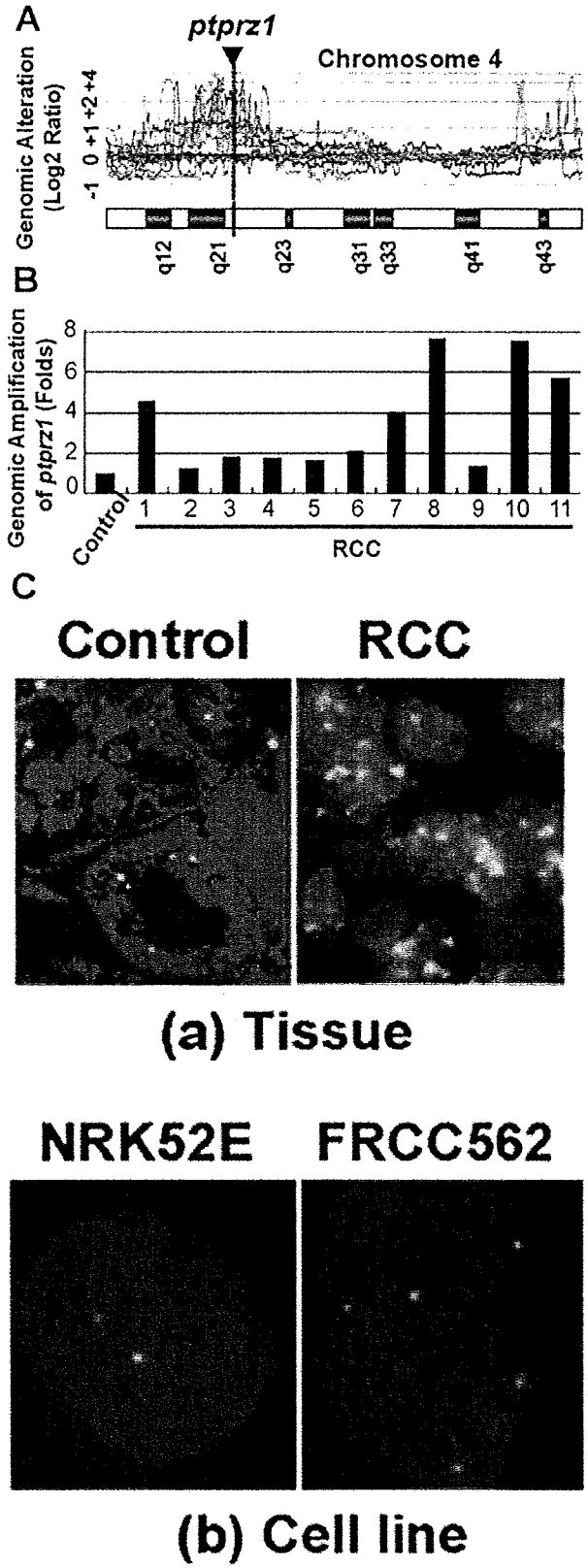

Figure 1. Gene amplification of *ptprz1* in Fe-NTA-induced RCCs. **A:** Array-based CGH analysis of 13 Fe-NTA-induced RCCs and 2 established cell lines, with profiles of chromosome 4 showing a broad peak at 4q22. Plus number at *y* axis indicates amplification at the chromosomal locus (log2 scale), whereas minus number indicates allelic loss, 0 is the normal 2N-state. Each color shows a different tumor. **B:** Copy number analysis by quantitative PCR. Eleven primary RCCs were analyzed. Means are shown after triplicate measurements that showed within 4% difference. Control, normal untreated kidney. **C:** Fluorescent *in situ* hybridization analysis of *ptprz1* genome. **a:** Paraffin-embedded specimen of Fe-NTA-induced RCC. Control, normal untreated kidney. **b:** Cell lines. Original magnification: ×160 (**a**); ×400 (**b**). Control kidney and NRK52E nontransformed rat renal tubular cell lines showed two or fewer (tissue) signals in the nucleus (nuclear counterstaining by propidium iodide) whereas RCC and FRCC-562 cell line showed more than two signals. Representative images are shown.

(Invitrogen) and Real-time PCR system 7300 (Applied Biosystems) were used. The glyceraldehyde 3-phosphate dehydrogenase gene was used as an internal control as previously described.[23] PCR reactions for each target and control genes were performed in triplicate. Primer sequences used were as follows: *ptprz1* based on NM_013080: forward, 5′-cccagctggtggttatgattcc-3′, and reverse, 5′-cgtgactttgaagctctctcgcaa-3′ (104-bp product); *cyclinD1* based on NM_171992: forward, 5′-tgtgccatccatgcggaaa-3′, and reverse, 5′-gacaagaaacggtccaggtagt-3′ (114-bp product); *c-myc* based on NM_012603: forward, 5′-tgtctatttggggacagtgttc-3′, and reverse, 5′-ctgttagcgaagctcacgtt-3′ (149-bp product); *c-jun* based on NM_021835: forward, 5′-gtgaaatgacagctgagtgtctg-3′, and reverse, 5′-gtcaacagtctggacttgtgg-3′ (141-bp product); *fra-1* based on NM_012953: forward, 5′-ctgctaagtgcagaaaccga-3′, and reverse, 5′-caaggcgttccttctgctt-3′ (129-bp product); and *CD44* based on NM_012924: forward, 5′-tttggtggcacacagcttg-3′, and reverse, 5′-atggaatacacctgcgtaacgg-3′ (104-bp product).

Ptprz1 mRNA In Situ *Hybridization*

Phosphate-buffered formaldehyde-fixed, paraffin-embedded specimens were used as previously described[25] using a DNA probe containing three repeats of ATT (underlined) at the 3′ end for T-T dimer formation with an exposure to 10 kJ/m^2 UV irradiation (5′-ctgagtatggcctcaaccagtgtgtcgtgaatgaagattattatt-3′). Minor modifications include pretreatment with 20 μg/ml proteinase K (37°C, 20 minutes), use of TDM-2 monoclonal antibody for T-T dimmer (1:4000 dilution),[26] and an application of tyramide signal amplification biotin system (PerkinElmer Japan, Yokohama, Japan) for sensitive detection.

Cell Culture

Cells were cultured in Dulbecco's modified Eagle's medium (GIBCO, Rockville, MD) containing 5% (NRK52E; Health Science Research Resources Bank, Osaka, Japan) or 10% (FRCC-001 and FRCC-562 cell lines[21]) fetal bovine serum, 100 U/ml penicillin, 100 μg/ml streptomycin, and 0.25 μg/ml amphotericin B at 37°C in a humidified 5% CO_2 incubator.

Expression Vectors and Transfection

Coding sequence of rat *ptprz1* (GenBank accession number NM_013080) was cloned by RT-PCR using cDNA of normal rat cerebrum as a substrate with the following primers: forward primer, 5′-ggggtaccccccacctggagat-

Table 1. Top 20 Up- and Down-Regulated Genes in Nonmetastatic RCCs

GenBank no.	Gene description	Fold change
Genes up-regulated in nonmetastatic RCCs		
NM_130741	*Lipocalin 2 (oncogene 24p3)*	3541.1
AW528743	*Major histocompatibility complex, class II, DQ α1*	282.1
AI137672	*CD69 antigen (p60, early T-cell activation antigen)*	184.8
AJ249701	*RT1 class Ib, locus Aw2*	140.1
NM_013080	*Protein tyrosine phosphatase, receptor-type, Z polypeptide 1*	101.8
NM_012812	*Cytochrome c oxidase subunit VIa polypeptide 2*	80.4
NM_133311	*Interleukin 24*	70.0
X73371	*Fc fragment of IgG, low affinity IIb, receptor (CD32)*	57.7
U05675	*Fibrinogen β-chain*	49.2
NM_133298	*Glycoprotein (transmembrane) nmb*	46.5
BE101834	*Laminin, β3*	43.7
NM_017222	*Solute carrier family 10, member 2*	39.9
AB020967	*Tribbles homolog 3 (Drosophila)*	39.1
NM_016994	*Complement component 3*	35.5
AI144754	*Rho family GTPase 1*	34.1
AF413572	*Protein kinase inhibitor β*	32.7
NM_022800	*Purinergic receptor P2Y, G-protein coupled, 12*	30.1
NM_012823	*Annexin A3*	26.9
NM_030845	*Chemokine (C-X-C motif) ligand 2*	26.5
NM_013110	*Interleukin 7*	24.4
Genes down-regulated in nonmetastatic RCCs		
X04280	*Calbindin 1, 28 kDa*	3769.1
D13906	*Aquaporin 2 (collecting duct)*	885.3
M27883	*Serine peptidase inhibitor, Kazal type 1*	471.1
NM_017111	*Solute carrier family 21, member 1*	455.1
L29403	*Potassium inwardly-rectifying channel, subfamily J, member 1*	430.5
NM_031703	*Aquaporin 3*	205.1
J04488	*Prostaglandin D2 synthase 21 kDa (brain)*	178.5
NM_017082	*Uromodulin (uromucoid, Tamm-Horsfall glycoprotein)*	176.1
NM_052802	*Kidney androgen regulated protein*	159.8
NM_017081	*Hydroxysteroid (11-β) dehydrogenase 2*	130.7
NM_016996	*Calcium-sensing receptor (hypocalciuric hypercalcemia 1, severe neonatal hyperparathyroidism)*	124.5
Z30663	*Chloride channel Kb*	117.0
BI288461	*ATPase, H+ transporting, lysosomal 56/58 kDa, V1 subunit B, isoform 1 (Renal tubular acidosis with deafness)*	113.0
AI235942	*Aquaporin 4*	112.2
BG377322	*Serpin peptidase inhibitor, clade C, member 1*	112.2
NM_022676	*Protein phosphatase 1, regulatory subunit 1A*	111.4
NM_012842	*Epidermal growth factor (β-urogastrone)*	97.7
AF189724	*Chemokine (C-X-C motif) ligand 12*	94.4
NM_012593	*Kallikrein 7 (chymotryptic, stratum corneum)*	89.9
NM_013097	*Deoxyribonuclease I*	81.6

gcgaatcctgca-3′ (*Kpn*I), and reverse primer, 5′-ggggGATATCcccctaccgtcaggtcatgggaagt-3′ (*Eco*RV). PCR products were digested with *Kpn*I and *Eco*RV (recognition sequences underlined) and subcloned into a mammalian expression vector pcDEF3,[27] which was transfected into NRK52E cell line with Lipofectamine 2000 (Invitrogen) and selected with 400 to 800 μg/ml G418.

siRNA Experiments

We designed siRNA oligonucleotides through siDirect software.[28] The target *ptprz1* sequence was 5′-AACCCTTATGCACCAACTAGAAA-3′ (6819–6841), and the siRNA was as follows: sense oligonucleotide, 5′-CCCUUAUGCACCAACUAGAAA-3′, and antisense, 5′-UCUAGUUGGUGCAUAAGGGUU-3′. The target *β-catenin* sequence was gagtcagcgacttgttcaaaact (1125 to 1147), and the siRNA was as follows: sense, 5′-GAGUCAGCGACUUGUUCAAAA-3′, and antisense, 5′-UUGAACAAGUCGCUGACUCGG-3′. The negative control (NegC; Naito1) was as follows: sense, 5′-GUACCGCACGUCAUUCGUAUC-3′, and antisense, 5′-UACGAAUGACGUGCGGUACGU-3′ (RNAi Co., Ltd, Tokyo, Japan). FRCC-001 and FRCC-562 were seeded in the complete medium without antibiotics to 30 to 50% confluence, transfected with siRNA oligonucleotides with Lipofectamine 2000, and incubated for 48 to 72 hours to confirm gene expression with quantitative RT-PCR and Western blot analysis.

Fractionation, Immunoprecipitation, and Western blot

These were done as previously described[22,29] except that 0.2 mmol/L Na_3VO_4, 50 mmol/L NaF, 1 mmol/L dithiothreitol, and 5.7 μg/ml aprotinine were included in the lysis buffer. Antibodies used were as follows: PTPRZ1

Table 2. Top 20 Up- and Down-Regulated Genes in Metastatic RCCs

GenBank no.	Gene description	Fold change
Genes up-regulated in metastatic RCCs		
NM_130741	*Lipocalin 2 (oncogene 24p3)*	2702.4
AI102790	*Branched chain aminotransferase 1, cytosolic*	1910.9
NM_133514	*Matrix metallopeptidase 10 (stromelysin 2)*	1112.8
M60616	*Matrix metallopeptidase 13 (collagenase 3)*	240.5
NM_133523	*Matrix metallopeptidase 3 (stromelysin 1, progelatinase)*	171.3
NM_013080	*Protein tyrosine phosphatase, receptor-type, Z polypeptide 1*	148.1
X73371	*Fc fragment of IgG, low affinity IIb, receptor (CD32)*	121.1
NM_012513	*Brain-derived neurotrophic factor*	106.2
NM_133298	*Glycoprotein (transmembrane) nmb*	94.4
AW528743	*Major histocompatibility complex, class II, DQ α1*	91.1
AJ249701	*RT1 class Ib, locus Aw2*	77.2
BI290559	*Microsomal glutathione S-transferase 2*	74.5
AI176732	*Triggering receptor expressed on myeloid cells 2*	72.5
NM_030845	*Chemokine (C-X-C motif) ligand 2*	60.1
NM_023021	*Potassium intermediate/small conductance calcium-activated channel, subfamily N, member 4*	59.3
BF545627	*Ets variant gene 4 (E1A enhancer binding protein, E1AF)*	58.5
NM_012912	*Activating transcription factor 3*	53.8
AF065147	*CD44 antigen (homing function and Indian blood group system)*	53.8
AF268593	*Integrin, αM*	50.6
AW527269	*Laminin, γ2*	49.5
Genes down-regulated in metastatic RCCs		
NM_052802	*Kidney androgen regulated protein*	3929.1
X04280	*Calbindin 1, 28 kDa*	1398.8
NM_017082	*Uromodulin (uromucoid, Tamm-Horsfall glycoprotein)*	1389.2
D13906	*Aquaporin 2 (collecting duct)*	1296.1
AB013455	*Solute carrier family 34 (sodium phosphate), member 1*	855.1
NM_013097	*Deoxyribonuclease I*	530.1
AI235942	*Aquaporin 4*	519.1
AI072107	*Aldo-keto reductase family 1, member C2*	471.1
BG377322	*Serpin peptidase inhibitor, clade C, member 1*	451.9
NM_012522	*cystathionine-β-synthase*	337.8
L29403	*Potassium inwardly-rectifying channel, subfamily J, member 1*	313.0
NM_017081	*Hydroxysteroid (11-β) dehydrogenase 2*	294.1
BE101119	*Parathyroid hormone receptor 1*	284.0
M27883	*Serine peptidase inhibitor, Kazal type 1*	270.6
NM_012619	*Phenylalanine hydroxylase*	265.0
NM_012842	*Epidermal growth factor (β-urogastrone)*	252.5
AA858962	*Retinol binding protein 4, plasma*	209.4
NM_031543	*Cytochrome P450, family 2, subfamily E, polypeptide 1*	199.5
NM_017111	*Solute carrier family 21, member 1*	186.1
BE097583	*Protein phosphatase 1, regulatory subunit 1A*	171.3

(clone 12; 1:100; BD Biosciences, San Jose, CA), β-catenin (clone 14; 1:100), phosphotyrosine (06-427; 1:100; Upstate, Lake Placid, NY), phospho-β-catenin (Ser33/37/Thr41; 1:1000; Cell Signaling Technology, Danvers, MA), and proliferating cell nuclear antigen (clone PC10; 1:3000; BioGenex, San Ramon, CA).

Immunohistochemistry and Immunocytochemistry

This was performed as previously described[22] with minor modifications. For the immunohistochemistry of paraffin-embedded specimens, the following antibodies were used: β-catenin (clone 196621; 1:100; R&D Systems, Inc., Minneapolis, MN), c-*myc* (clone 9E10; 1:50; Santa Cruz Biotechnology, Inc., Santa Cruz, CA), and cyclin D1 (SP4; 1:50; NeoMarkers, Inc., Fremont, CA). Antigen retrieval was performed by autoclaving at 121°C for 15 minutes in 10 mmol/L citrate buffer at pH 6.0. For the immunocytochemistry, cells grown on Lab-Tek II Chamber Slide w/Cover (Nalge Nunc International, Naperville, IL) at approximately 70% confluence were fixed with cold methanol for 10 minutes, followed by permeation with 0.5% Triton X-100 for 10 minutes at room temperature. The same antibody against β-catenin was used at a dilution of 1:100. A tyramide signal amplification biotin system (PerkinElmer) was used to increase sensitivity. FITC-avidin and nuclear counterstaining with propidium iodide were used. Images were analyzed with confocal laser microscopy (Fluoview, Olympus, Osaka, Japan).

Cell Proliferation Analysis

Cells were seeded in a six-well plate at first in Dulbecco's modified Eagle's medium with serum but without antibiotics. After 24 hours, siRNA oligonucleotides for *ptprz1* were transfected, followed by cell counting starting from 24 hours after transfection to the fifth day in triplicate.

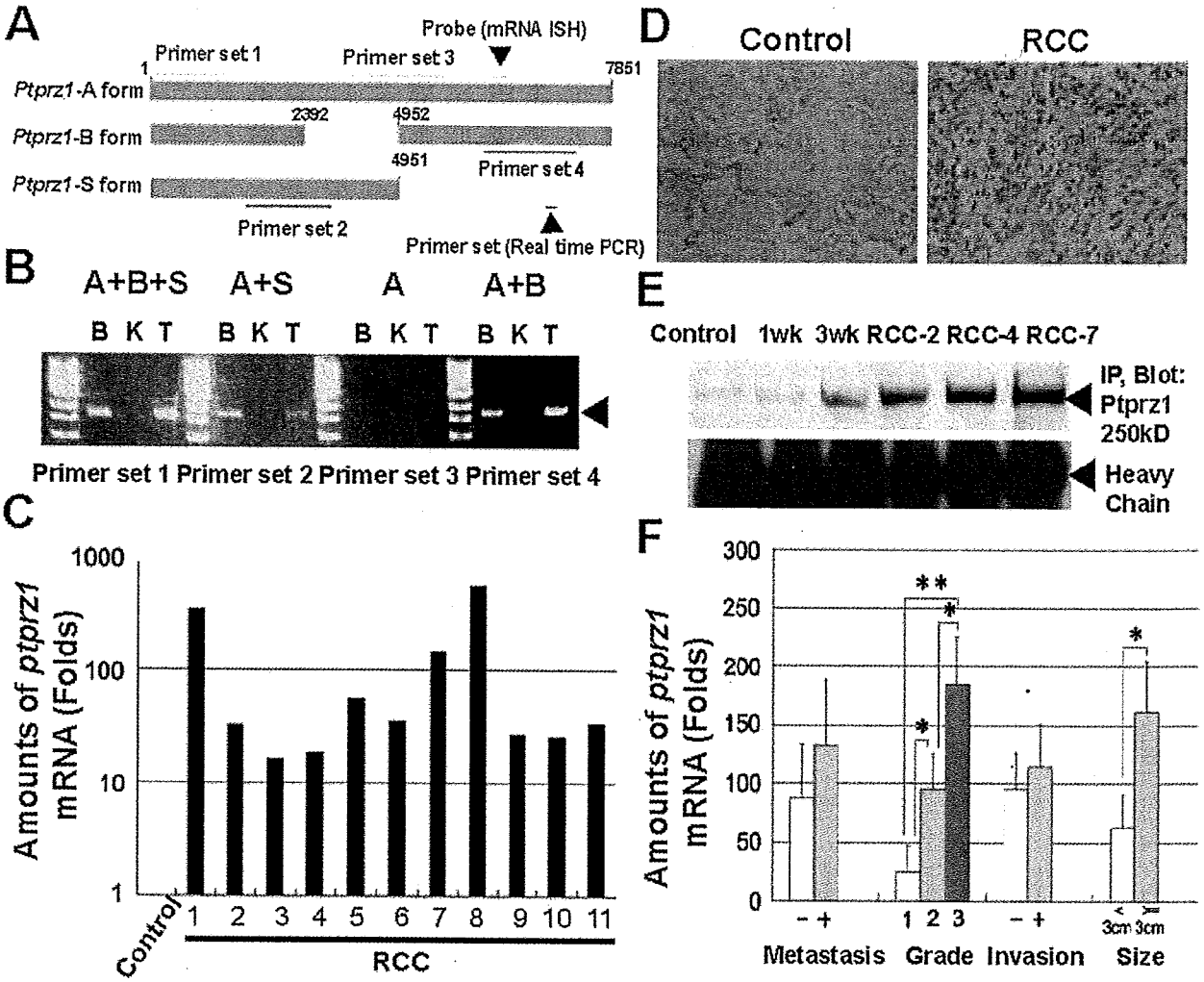

Figure 2. PTPRZ1 Isoform B is major in Fe-NTA-induced RCCs and is associated with tumor grade and size. **A:** Location of primers and mRNA hybridization probes in the *ptprz1* cDNA. Primer set 1 is common to all of the isoforms (A, B, and S); primer set 2 is specific to A and S isoforms; primer set 3 is specific only to A isoform; primer set 4 is specific to A and B isoforms. **B:** RT-PCR analysis. B, brain; K, control kidney; T, Fe-NTA-induced RCC. Control kidney expressed undetectable amount of *ptprz1* mRNA; major isoform in RCC was B isoform. A representative analysis is shown. **C:** Levels of *ptprz1* expression. Registered numbers of RCCs in Figure 1B and **C** and **E** in this figure correspond to each other. Means are shown after triplicate measurements that showed within 11% difference. Control, normal untreated kidney. **D:** mRNA is situ hybridization analysis. RCC cells expressed abundant *ptprz1* mRNA whereas control renal proximal tubules showed faint expression (original magnification, ×80). **E:** Protein levels of *ptprz1*. For specific and sensitive detection, immunoprecipitation was performed. Fe-NTA-induced RCCs as well as kidney after chronic oxidative stress by Fe-NTA for 3 weeks showed induction of PTPRZ1. **F:** Association of *ptprz1* mRNA levels with tumor parameters. Tumor grade and size revealed a proportional association with *ptprz1* expression (means ± SEM, $N = 3$–10; $^*P < 0.05$; $^{**}P < 0.01$).

Statistical Analysis

Statistical analyses were performed with an unpaired *t*-test in which $P < 0.05$ was considered as statistically significant.

Results

Array-Based CGH and Gene Expression Microarray Analyses Identified ptprz1 Amplification and Overexpression

We analyzed 13 Fe-NTA-induced rat RCCs and 2 cell lines established from them with array-based comparative genomic hybridization analyses. Chromosome 4q22 revealed the highest incidence of common genomic amplification among the 20 autosomes and X chromosome (Figure 1A). Detailed reports of the whole CGH analyses will be published elsewhere (S. Akatsuka and S. Toyokuni, unpublished data). At the same time, we analyzed four primary RCCs (two nonmetastatic and two metastatic tumors) with gene expression microarray analyses (Tables 1 and 2; Gene Expression Omnibus accession number GSE7625). With the expression microarray analyses, *ptprz1* was the fifth and sixth in the lists of up-regulated genes in nonmetastatic and metastatic RCCs, respectively, and was present on chromosome 4q22. Thus, we decided to focus on *ptprz1* based on these two sets of data. Quantitative PCR analyses revealed that 7 of 11 primary RCCs

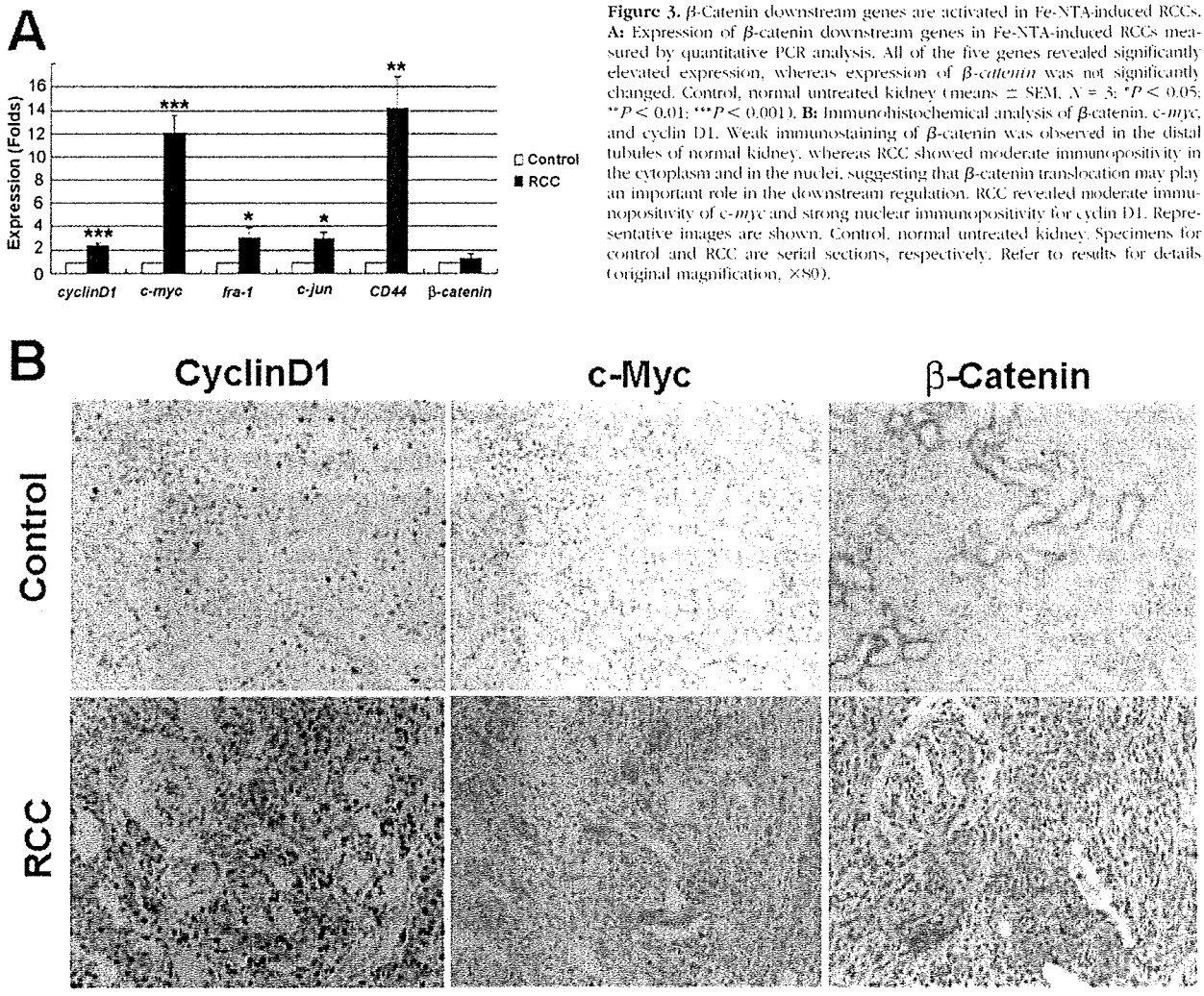

Figure 3. β-Catenin downstream genes are activated in Fe-NTA-induced RCCs. **A:** Expression of β-catenin downstream genes in Fe-NTA-induced RCCs measured by quantitative PCR analysis. All of the five genes revealed significantly elevated expression, whereas expression of *β-catenin* was not significantly changed. Control, normal untreated kidney (means ± SEM, $N = 3$; $^{*}P < 0.05$; $^{**}P < 0.01$; $^{***}P < 0.001$). **B:** Immunohistochemical analysis of β-catenin, *c-myc*, and cyclin D1. Weak immunostaining of β-catenin was observed in the distal tubules of normal kidney, whereas RCC showed moderate immunopositivity in the cytoplasm and in the nuclei, suggesting that β-catenin translocation may play an important role in the downstream regulation. RCC revealed moderate immunopositivity of *c-myc* and strong nuclear immunopositivity for cyclin D1. Representative images are shown. Control, normal untreated kidney. Specimens for control and RCC are serial sections, respectively. Refer to results for details (original magnification, ×80).

showed genomic amplification of *ptprz1* with 5 tumors showing more than fourfold increase (Figure 1B). We used fluorescence *in situ* hybridization analyses to confirm the amplification. In high-copy number tumors, a significantly increased number of signals were observed, whereas control cells showed two or less. Data obtained from cell lines were clearer because of the optimal fixation (Figure 1C).

Overexpression of ptprz1 Is Mainly of the B Isoform and Is Associated with Tumor Grade and Size

To differentiate three isoforms of *ptprz1* reported,[24] we designed specific primers for RT-PCR analyses (Figure 2A) and found that the B isoform is the major isoform in tumors (Figure 2B). Thus, we focused on the B isoform. All of the primary RCCs examined showed 16~552-fold increases in *ptprz1* expression in comparison with that of a normal untreated kidney (Figure 2C). *In situ* hybridization analyses confirmed the results, revealing abundant staining in the cytoplasm of RCC cells (Figure 2D). At the protein level, repeated treatment of Fe-NTA for 3 weeks increased PTPRZ1 with a further increase in tumors (Figure 2E). We compared four parameters (pulmonary metastasis, grade, peritoneal invasion and tumor size) of the primary RCCs with mRNA levels and found that morphological grade[13] and size of the tumor were proportionally associated (Figure 2F).

Overexpression of ptprz1 Activates β-catenin Pathway

Because network analysis of gene expression microarray data pointed out the involvement of the β-catenin signaling pathway, we studied the status of β-catenin and its downstream genes such as *cyclinD1*, *c-jun*, *c-myc*, fra-1, and *CD44* with quantitative PCR and immunohistochemistry. In the Fe-NTA-induced RCCs analyzed, all of the five *β-catenin* downstream genes were overexpressed, whereas *β-catenin* expression was not significantly increased (Figure 3A). Paraffin-embedded specimens were used for immunohistochemistry. Weak immunostaining of β-catenin was observed in the distal tubules of

normal kidney but not in the proximal tubules where Fe-NTA-induced RCCs are believed to be originated, whereas RCCs showed moderate immunopositivity in the cytoplasm and weak to moderate immunopositivity in the nuclei, suggesting that β-catenin abundance and translocation may play an important role in the downstream regulation. RCCs revealed weak to moderate immunopositivity of c-*myc*, and all of the RCCs showed strong nuclear immunopositivity for cyclin D1 (Figure 3B). These results strongly indicated the involvement of *β-catenin* pathway in the molecular mechanism of Fe-NTA-induced renal carcinogenesis. To demonstrate the causal relationship of *ptprz1* and *β-catenin*-downstream genes, we used cell culture systems thereafter.

Firstly, we evaluated the interaction of PTPRZ1 and β-catenin by the use of a nontransformed rat renal tubular cell line (NRK52E) and two Fe-NTA-induced rat RCC cell lines (FRCC-001 and FRCC-562).[21] We observed the presence of PTPRZ1 and the interaction of the two proteins only in the RCC cell lines (Figure 4A). Next, we performed *ptprz1* transfection to NRK52E cells and found that nuclear dephosphorylated β-catenin was significantly increased and that tyrosine, but not serine/threonine, residues were the target amino acid for dephosphorylation (Figure 4, B and C). This was accompanied by the expressional increase in the β-catenin downstream target genes such as *cyclinD1*, *c-jun*, *c-myc*, fra-1, and *CD44*, which was abolished with the simultaneous transfection of *β-catenin* siRNA, demonstrating that PTPRZ1 is upstream of β-catenin (Figure 5A). Furthermore, we performed an siRNA transfection study of *ptprz1* in the two RCC cell lines. With this procedure, nuclear β-catenin was significantly decreased with a relative increase in phosphorylated β-catenin at tyrosine (Figure 4B). This was accompanied by a marked expressional decrease in the β-catenin target genes (Figure 5, B and C). As seen by the nuclear presence of unphosphorylated β-catenin and the expressional increase in β-catenin downstream target genes, the endpoints were associated with cell proliferation and the levels of proliferating cell nuclear antigen (Figure 5, D–G).

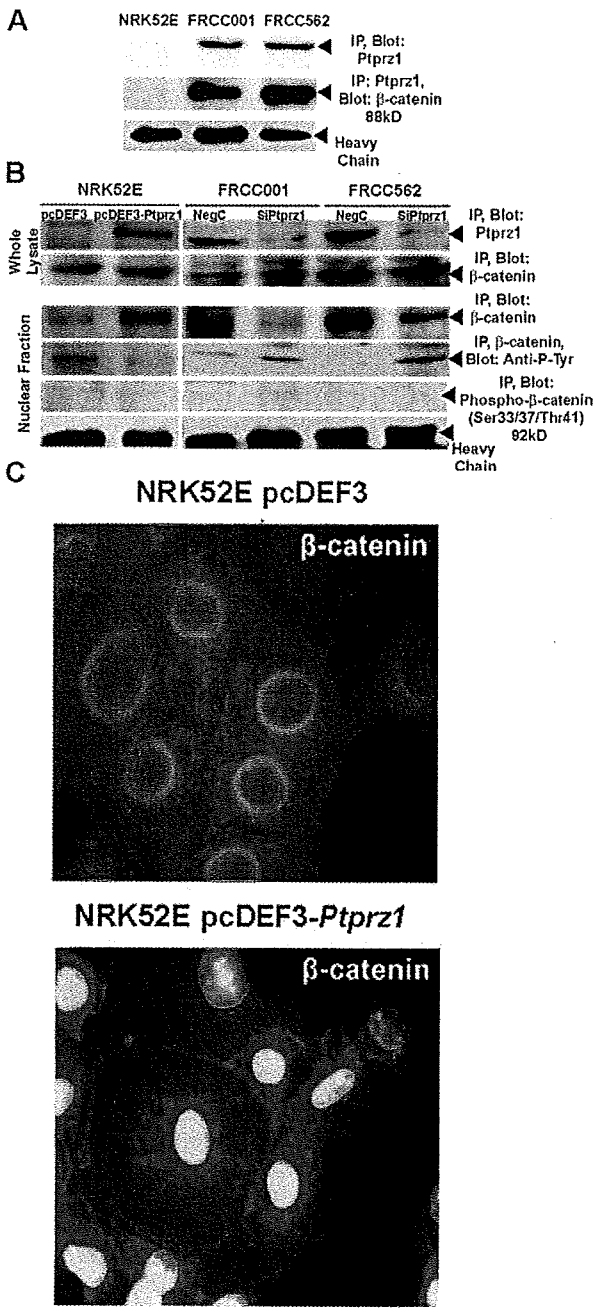

Figure 4. PTPRZ1 dephosphorylates tyrosine residues of β-catenin for nuclear translocation. **A:** Interaction of PTPRZ1 and β-catenin. NRK52E, nontransformed rat renal tubular cell line; FRCC-001 and FRCC-562 cell lines established from Fe-NTA-induced rat RCCs. PTPRZ1 is overexpressed only in FRCC cell lines and is associated with β-catenin. **B:** Tyrosine, but not serine or threonine, residues of β-catenin are the substrate of PTPRZ1 in association with nuclear translocation of β-catenin. **C:** Transfection of *ptprz1* induces nuclear translocation of β-catenin (fluorescein isothiocyanate; nuclear counterstaining by propidium iodide; original magnification, ×400).

Discussion

The biological significance of oxidative stress resulting from the continuous consumption of oxygen has become more and more important with respect to the increase in human lifetime. Oxidative stress can induce two completely different outcomes depending on the extent and the situation, namely cell death or proliferation.[30,31] Cancer, one of the major causes of mortalities in the world, may be interpreted as a futile evolutionary effort on cellular proliferation under the given environment. Here, we undertook to obtain the responsible genetic alterations during carcinogenesis out of the selective process via chronic oxidative stress. In the established animal model of oxidative stress-induced carcinogenesis,[5,12,32] we found for the first time that oxidative stress amplifies certain specific chromosomal regions *in vivo* using array-based comprehensive CGH analysis.

Previously, Hunt et al[33] reported that chronic exposure of HA1 fibroblasts to increasing concentrations of H_2O_2 or O_2 causes *catalase* gene amplification with increased amounts of message and protein and also discussed the results in association with the resistance against chemotherapeutic drugs in which pharmacological effects depend on oxidative stress. Our present findings are dis-

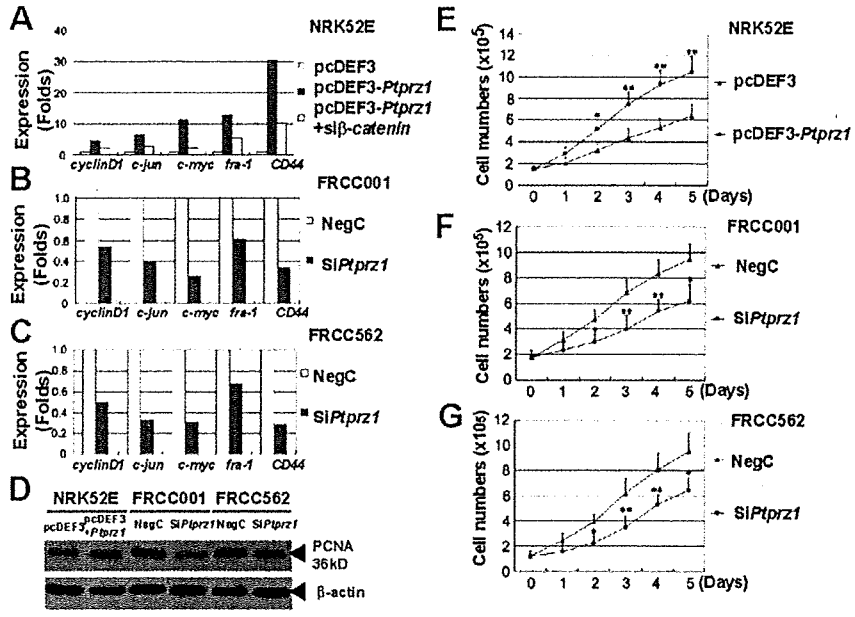

Figure 5. Function of β-catenin is regulated by ptprz1. **A–C:** Expression of β-catenin downstream genes is dependent on the levels of *ptprz1* expression. In NRK52E cells (**A**), transfection of *ptprz1* caused induction of β-catenin downstream genes, and this was reversed by specific knockdown of β-*catenin*. In FRCC-001 (**B**) and FRCC-562 (**C**) cells, specific knockdown of *ptprz1* caused down-regulation of β-catenin downstream genes. In **A–C**, means are shown after duplicate measurements that showed within 12% difference. **D:** Expressional levels of *ptprz1* are associated with protein levels of proliferating nuclear antigen (PCNA), a marker of cell proliferation. **E–G:** Expression levels of *ptprz1* are associated with cell proliferation. NegC, negative control (means ± SEM, $N = 3$; $^{*}P < 0.05$, $^{**}P < 0.01$).

tinct from theirs in the following contexts: 1) gene amplification occurred in nonimmortalized cells *in vivo* at multiple different locations, suggesting either the presence of episomal/double minute chromosomes or multiple integration, and 2) the amplified genes were not necessarily associated with resistance to chronic oxidative stress. This is of note, considering the fact that a certain population of human cancers presents gene amplification, including the HER-2/neu proto-oncogene in breast cancers.[3,4,35] The results indicate that persistent oxidative stress is one of the driving forces for gene amplification.

We have integrated the results from CGH analysis and gene expression microarray analysis and focused on *ptprz1* (also called protein tyrosine phosphatase ζ or receptor protein tyrosine phosphatase β) in the present study. All of the 13 Fe-NTA-induced RCCs and two cell lines showed overexpression of *ptprz1*, whereas approximately one-half of them acquired gene amplification. Overexpression of *ptprz1* was observed after as early as 3 weeks of persistent oxidative stress. These results suggest that overexpression and the possible associated open chromatin structure are necessary but probably not enough for the gene amplification. Other possible factors involved are neighbor gene effect and chromosome territory. It is now believed that genomic DNA corresponding to certain chromosomes shares a rather fixed stereographical position in nuclei even in interphase.[36,37] Thus, a three-dimensional understanding of the neighboring genes would be necessary to understand fully the mechanism of gene amplification. Recently, we found that there are fragile sites (oxidative DNA base modifications) against oxidative stress in the genome using a novel method of DNA immunoprecipitation.[15] Genome replication, repair, and recombination should further be considered to elucidate the gene-amplifying mechanism. This carcinogenesis model presents an ideal material for further investigation.

We performed functional analyses on *ptprz1* expression using an untransformed rat renal tubular cell line and two cell lines derived from Fe-NTA-induced rat RCCs. *Ptprz1* mRNA was abundantly expressed in the cerebrum and cerebellum in rats but was extremely low in the heart, lung, liver, kidney, and stomach (approximately 1/100; data not shown). The major isoform of *ptprz1* in this model was the B isoform, one of the major isoforms in adult brain,[24] and chronic oxidative stress increased the expression of *ptprz1* in the kidney. So far, we have not yet identified the core consensus sequences in the promoter region of *ptprz1* that responded to chronic oxidative stress, but hypoxia-inducible factor-2 could be involved in this process because recent study suggested that hypoxia-inducible factor-2 overexpression is important in the development of renal carcinoma in patients with von Hippel Lindau tumor suppressor protein.[38,39] The A isoform was present during the prenatal period of rat brain and decreased rapidly after birth. Isoform B is the most deficient in the modification with carbohydrates among the three forms but retains cytoplasmic phosphatase domain.[24] With this information, we decided to identify the signal pathways involved downstream of the B isoform.

We focused on the β-catenin pathway because network analysis of the gene expression microarray data on RCCs indicated the involvement of this pathway. The β-catenin transcription coactivator is a key transducer of the Wnt signaling in the canonical pathway. In the absence of Wnt, a multiprotein destruction complex containing glycogen synthetase β, axin, disheveled, casein kinase 1, and adenomatous polyposis coli facilitates β-catenin degradation by the proteasome.[40] In our results, we add a novel switching mechanism of this pathway.

In the previous reports, function of *ptprz1* in cancer has been controversial. Meng et al reported that pleiotrophin,[41] a platelet-derived growth factor-inducible cytokine and a proto-oncogene, interacts with PTPRZ1 in a

glioblastoma cell line (U373-MG) to inactivate its catalytic activity, leading to an increase in the tyrosine phosphorylation levels of β-catenin.[42] In contrast, it was recently reported that targeting of PTPRZ1 with a monoclonal antibody delays tumor growth in a glioblastoma model.[43,44] We found that modulation of tyrosine phosphorylation in β-catenin controlled by *ptprz1* is a key process of the *β-catenin* pathway in this model. Activation of neither pleiotrophin nor Wnt signaling (Wnt2b, Wnt4, or Wnt5a) was observed (GEO accession number GSE7625; data not shown), but β-catenin was translocated to the nucleus, and the downstream target genes of β-catenin were activated in this model. This type of activation appears to be cell specific, considering the fact that normal renal proximal tubular cells show undetectable levels of *ptprz1* mRNA. *Ptprz1* has recently been identified as important in the recovery from demyelinating lesions,[45] is associated with susceptibility to VacA of *Helicobacter pylori* in murine stomach,[46] and was up-regulated after hypoxia-inducible factor-2α transfection in HEK293T (adenovirus-transformed human fetal kidney cells).[47] It is possible to interpret from our results that cancer cells use metabolisms similar to fetal tissues in that they proliferate rapidly in a hypoxic environment.[48] 2-^{18}F-fluoro-2-deoxy-D-glucose, a radioactive derivative of glucose, is widely used for the diagnosis of cancer, based on the increased glucose consumption of cancer cells.[49] Our previous observation in this carcinogenesis model that thioredoxin-binding protein-2 is inactivated via methylation of the promoter region, leading to the activation of glycolytic pathway via thioredoxin system,[22,50] supports this hypothesis.

In conclusion, we show for the first time, to our knowledge, that chronic oxidative stress causes gene amplification *in vivo* through a combination of comprehensive array-based CGH and gene expression microarrray analyses in an oxidative stress-induced carcinogenesis model. Furthermore, we found a novel β-catenin signal activation mechanism through overexpression of *ptprz1* protein tyrosine phosphatase. Oxidative stress is closely associated not only with carcinogenesis but also with tumor biology.[10,31] We believe that oxidative stress, especially of a chronic nature, presents an environment for competitive cell proliferation rather than cooperative cell survival, giving opportunities for selection. We do not know at present whether activation of the β-catenin pathway through *ptprz1* amplification is a specific event only in renal tubular cells or oxidative stress-induced carcinogenesis. Because gene amplification in human cancer is often associated with poor prognosis[51] and is a mechanism of resistance to therapies,[52] this animal model confers an intriguing opportunity not only for the elucidation of carcinogenesis toward cancer prevention but also of therapeutic resistance.

Acknowledgments

We thank Dr. Masaharu Noda (National Institute for Basic Biology, Okazaki, Japan) for discussion. The pcDEF3 expression vector was a kind gift from Dr. Gerome A Langer (Robert Wood Johnson Medical School, Piscataway, NJ).

References

1. Halliwell B, Gutteridge JMC: Free Radicals in Biology and Medicine. New York, Oxford University Press, 2007
2. Iuchi K, Ichimiya A, Akashi A, Mizuta T, Lee Y, Tada H, Mori T, Sawamura K, Lee Y, Furuse K, Yamamoto S, Aozasa K: Non-Hodgkin's lymphoma of the pleural cavity developing from long-standing pyothorax. Cancer 1987, 60:1771–1775
3. Uemura N, Okamoto S, Yamamoto S, Matsumura N, Yamaguchi S, Yamakido M, Taniyama K, Sasaki N, Schlemper R: Helicobacter pylori infection and the development of gastric cancer. N Engl J Med 2001, 345:784–789
4. Eaden J, Abrams K, Mayberry J: The risk of colorectal cancer in ulcerative colitis: a meta-analysis. Gut 2001, 48:526–535
5. Toyokuni S: Iron-induced carcinogenesis: the role of redox regulation. Free Radic Biol Med 1996, 20:553–566
6. Elmberg M, Hultcrantz R, Ekbom A, Brandt L, Olsson S, Olsson R, Lindgren S, Loof L, Stal P, Wallerstedt S, Almer S, Sandberg-Gertzen H, Askling J: Cancer risk in patients with hereditary hemochromatosis and in their first-degree relatives. Gastroenterology 2003, 125:1733–1741
7. Hodgson J, Darnton A: The quantitative risks of mesothelioma and lung cancer in relation to asbestos exposure. Ann Occup Hyg 2000, 44:565–601
8. Nishigori C, Hattori Y, Toyokuni S: Role of reactive oxygen species in skin carcinogenesis. Antioxid Redox Signal 2004, 6:561–570
9. Preston D, Kusumi S, Tomonaga M, Izumi S, Ron E, Kuramoto A, Kamada N, Dohy H, Matsui T, Nonaka H, Thompson DE, Soda M, Mabuchi K: Cancer incidence in atomic bomb survivors: Part III. Leukemia, lymphoma and multiple myeloma, 1950–1987. Radiat Res 1994, 137:S68–S97
10. Toyokuni S, Okamoto K, Yodoi J, Hiai H: Persistent oxidative stress in cancer. FEBS Lett 1995, 358:1–3
11. Li JL, Okada S, Hamazaki S, Ebina Y, Midorikawa O: Subacute nephrotoxicity and induction of renal cell carcinoma in mice treated with ferric nitrilotriacetate. Cancer Res 1987, 47:1867–1869
12. Ebina Y, Okada S, Hamazaki S, Ogino F, Li JL, Midorikawa O: Nephrotoxicity and renal cell carcinoma after use of iron- and aluminum-nitrilotriacetate complexes in rats. J Natl Cancer Inst 1986, 76:107–113
13. Nishiyama Y, Suwa H, Okamoto K, Fukumoto M, Hiai H, Toyokuni S: Low incidence of point mutations in H-, K- and N-ras oncogenes and p53 tumor suppressor gene in renal cell carcinoma and peritoneal mesothelioma of Wistar rats induced by ferric nitrilotriacetate. Jpn J Cancer Res 1995, 86:1150–1158
14. Toyokuni S, Mori T, Dizdaroglu M: DNA base modifications in renal chromatin of Wistar rats treated with a renal carcinogen, ferric nitrilotriacetate. Int J Cancer 1994, 57:123–128
15. Akatsuka S, Aung TT, Dutta KK, Jiang L, Lee WH, Liu YT, Onuki J, Shirase T, Yamasaki K, Ochi H, Naito Y, Yoshikawa T, Kasai H, Tominaga Y, Sakumi K, Nakabeppu Y, Kawai Y, Uchida K, Yamasaki A, Tsuruyama T, Yamada Y, Toyokuni S: Contrasting genome-wide distribution of 8-hydroxyguanine and acrolein-modified adenine during oxidative stress-induced renal carcinogenesis. Am J Pathol 2006, 169:1328–1342
16. Toyokuni S, Uchida K, Okamoto K, Hattori-Nakakuki Y, Hiai H, Stadtman ER: Formation of 4-hydroxy-2-nonenal-modified proteins in the renal proximal tubules of rats treated with a renal carcinogen, ferric nitrilotriacetate. Proc Natl Acad Sci USA 1994, 91:2616–2620
17. Toyokuni S, Luo XP, Tanaka T, Uchida K, Hiai H, Lehotay DC: Induction of a wide range of C_{2-12} aldehydes and C_{7-12} acyloins in the kidney of Wistar rats after treatment with a renal carcinogen, ferric nitrilotriacetate. Free Radic Biol Med 1997, 22:1019–1027
18. Zhang D, Okada S, Yu Y, Zheng P, Yamaguchi R, Kasai H: Vitamin E inhibits apoptosis: DNA modification, and cancer incidence induced by iron-mediated peroxidation in Wistar rat kidney. Cancer Res 1997, 57:2410–2414
19. Tanaka T, Iwasa Y, Kondo S, Hiai H, Toyokuni S: High incidence of allelic loss on chromosome 5 and inactivation of $p15^{INK4B}$ and $p16^{INK4A}$ tumor suppressor genes in oxystress-induced renal cell carcinoma of rats. Oncogene 1999, 18:3793–3797
20. Hiroyasu M, Ozeki M, Kohda H, Echizenya M, Tanaka T, Hiai H, Toyokuni S: Specific allelic loss of $p16^{INK4A}$ tumor suppressor gene

after weeks of iron-mediated oxidative damage during rat renal carcinogenesis. Am J Pathol 2002, 160:419–424
21. Tanaka T, Akatsuka S, Ozeki M, Shirase T, Hiai H, Toyokuni S: Redox regulation of annexin 2 and its implications for oxidative stress-induced renal carcinogenesis and metastasis. Oncogene 2004, 23:3980–3989
22. Dutta KK, Nishinaka Y, Masutani H, Akatsuka S, Aung TT, Shirase T, Lee W-H, Hiai H, Yodoi J, Toyokuni S: Two distinct mechanisms for loss of thioredoxin-biding protein-2 in oxidative stress-induced renal carcinogenesis. Lab Invest 2005, 85:798–807
23. Lee W, Akatsuka S, Shirase T, Kumar Dutta K, Jiang L, Liu Y, Onuki J, Yamada Y, Okawa K, Wada Y, Watanabe A, Kohro T, Noguchi N, Toyokuni S: α-Tocopherol induces calnexin in renal tubular cells: another protective mechanism against free radical-induced cellular damage. Arch Biochem Biophys 2006, 453:168–178
24. Nishiwaki T, Maeda N, Noda M: Characterization and developmental regulation of proteoglycan-type protein tyrosine phosphatase zeta/RPTPbeta isoforms. J Biochem (Tokyo) 1998, 123:458–467
25. Yamamoto-Fukuda T, Aoki D, Hishikawa Y, Kobayashi T, Takahashi H, Koji T: Possible involvement of keratinocyte growth factor and its receptor in enhanced epithelial-cell proliferation and acquired recurrence of middle-ear cholesteatoma. Lab Invest 2003, 83:123–136
26. Hattori Y, Nishigori C, Tanaka T, Uchida K, Nikaido O, Osawa T, Hiai H, Imamura S, Toyokuni S: 8-Hydroxy-2′-deoxyguanosine is increased in epidermal cells of hairless mice after chronic UVB exposure. J Invest Dermatol 1996, 107:733–737
27. Goldman L, Cutrone E, Kotenko S, Krause C, Langer J: Modifications of vectors pEF-BOS, pcDNA1 and pcDNA3 result in improved convenience and expression. Biotechniques 1996, 21:1013–1015
28. Naito Y, Yamada T, Ui-Tei K, Morishita S, Saigo K: siDirect: highly effective, target-specific siRNA design software for mammalian RNA interference. Nucleic Acids Res 2004, 32:W124–W129
29. Toyokuni S, Kawaguchi W, Akatsuka S, Hiroyasu M, Hiai H: Intermittent microwave irradiation facilitates antigen-antibody reaction in Western blot analysis. Pathol Int 2003, 53:259–261
30. Toyokuni S, Akatsuka S: What has been learned from the studies of oxidative stress-induced carcinogenesis: proposal of the concept of oxygenomics. J Clin Biochem Nutr 2006, 39:3–10
31. Toyokuni S, Akatsuka S: Pathological investigation of oxidative stress in the postgenomic era. Pathol Int 2007, 57:461–473
32. Okada S: Iron-induced tissue damage and cancer: the role of reactive oxygen free radicals. Pathol Int 1996, 46:311–332
33. Hunt C, Sim J, Sullivan S, Featherstone T, Golden W, Von Kapp-Herr C, Hock R, Gomez R, Parsian A, Spitz D: Genomic instability and catalase gene amplification induced by chronic exposure to oxidative stress. Cancer Res 1998, 58:3986–3992
34. Slamon D, Clark G, Wong S, Levin W, Ullrich A, McGuire W: Human breast cancer: correlation of relapse and survival with amplification of the HER-2/neu oncogene. Science 1987, 235:177–182
35. Albertson D: Gene amplification in cancer. Trends Genet 2006, 22:447–455
36. Cremer T, Cremer C: Chromosome territories, nuclear architecture and gene regulation in mammalian cells. Nat Rev Genet 2001, 2:292–301
37. Meaburn KJ, Misteli T: Chromosome territories. Nature 2007, 445:379–381
38. Maranchie J, Vasselli J, Riss J, Bonifacino J, Linehan W, Klausner R: The contribution of VHL substrate binding and HIF1-α to the phenotype of VHL loss in renal cell carcinoma. Cancer Cell 2002, 1:247–255
39. Kondo K, Klco J, Nakamura E, Lechpammer M, Kaelin W: Inhibition of HIF is necessary for tumor suppression by the von Hippel-Lindau protein. Cancer Cell 2002, 1:237–246
40. Clevers H: Wnt/beta-catenin signaling in development and disease. Cell 2006, 127:469–480
41. Chauhan A, Li Y, Deuel T: Pleiotrophin transforms NIH 3T3 cells and induces tumors in nude mice. Proc Natl Acad Sci USA 1993, 90:679–682
42. Meng K, Rodriguez-Pena A, Dimitrov T, Chen W, Yamin M, Noda M, Deuel T: Pleiotrophin signals increased tyrosine phosphorylation of beta-catenin through inactivation of the intrinsic catalytic activity of the receptor-type protein tyrosine phosphatase beta/zeta. Proc Natl Acad Sci USA 2000, 97:2603–2608
43. Foehr E, Lorente G, Kuo J, Ram R, Nikolich K, Urfer R: Targeting of the receptor protein tyrosine phosphatase beta with a monoclonal antibody delays tumor growth in a glioblastoma model. Cancer Res 2006, 66:2271–2278
44. Ulbricht U, Eckerich C, Fillbrandt R, Westphal M, Lamszus K: RNA interference targeting protein tyrosine phosphatase zeta/receptor-type protein tyrosine phosphatase beta suppresses glioblastoma growth in vitro and in vivo. J Neurochem 2006, 98:1497–1506
45. Harroch S, Furtado G, Brueck W, Rosenbluth J, Lafaille J, Chao M, Buxbaum J, Schlessinger J: A critical role for the protein tyrosine phosphatase receptor type Z in functional recovery from demyelinating lesions. Nat Genet 2002, 32:411–414
46. Fujikawa A, Shirasaka D, Yamamoto S, Ota H, Yahiro K, Fukada M, Shintani T, Wada A, Aoyama N, Hirayama T, Fukamachi H, Noda M: Mice deficient in protein tyrosine phosphatase receptor type Z are resistant to gastric ulcer induction by VacA of Helicobacter pylori. Nat Genet 2003, 33:375–381
47. Wang V, Davis D, Haque M, Huang L, Yarchoan R: Differential gene up-regulation by hypoxia-inducible factor-1α and hypoxia-inducible factor-2α in HEK293T cells. Cancer Res 2005, 65:3299–3306
48. Nodwell A, Carmichael L, Ross M, Richardson B: Placental compared with umbilical cord blood to assess fetal blood gas and acid-base status. Obstet Gynecol 2005, 105:129–138
49. Endo K, Oriuchi N, Higuchi T, Iida Y, Hanaoka H, Miyakubo M, Ishikita T, Koyama K: PET and PET/CT using ^{18}F-FDG in the diagnosis and management of cancer patients. Int J Clin Oncol 2006, 11:286–296
50. Oka S, Liu W, Masutani H, Hirata H, Shinkai Y, Yamada S, Yoshida T, Nakamura H, Yodoi J: Impaired fatty acid utilization in thioredoxin binding protein-2 (TBP-2)-deficient mice: a unique animal model of Reye syndrome. FASEB J 2005, 147:733–743
51. Chung C, Ely K, McGavran L, Varella-Garcia M, Parker J, Parker N, Jarrett C, Carter J, Murphy B, Netterville J, Burkey B, Sinard R, Cmelak A, Levy S, Yarbrough W, Slebos R, Hirsch F: Increased epidermal growth factor receptor gene copy number is associated with poor prognosis in head and neck squamous cell carcinomas. J Clin Oncol 2006, 24:4170–4176
52. Cullen K, Newkirk K, Schumaker L, Aldosari N, Rone J, Haddad B: Glutathione S-transferase pi amplification is associated with cisplatin resistance in head and neck squamous cell carcinoma cell lines and primary tumors. Cancer Res 2003, 63:8097–8102

5-Aminosalicylic Acid Given in the Remission Stage of Colitis Suppresses Colitis-Associated Cancer in a Mouse Colitis Model

Ikuko Ikeda,[1] Ayako Tomimoto,[1] Koichiro Wada,[3] Toshio Fujisawa,[1] Koji Fujita,[1] Kyoko Yonemitsu,[1] Yuichi Nozaki,[1] Hiroki Endo,[1] Hirokazu Takahashi,[1] Masato Yoneda,[1] Masahiko Inamori,[1] Kensuke Kubota,[1] Satoru Saito,[1] Yoji Nagashima,[2] Hitoshi Nakagama,[4] and Atsushi Nakajima[1]

Abstract **Purpose:** The risk of colorectal cancer is increased in patients with inflammatory bowel diseases, especially those with ulcerative colitis (UC). Although 5-aminosalicylic acid (5-ASA) is widely used in the treatment of UC to suppress the colitic inflammation, no studies have been conducted to examine the chemopreventive effect of 5-ASA, given in the remission phase of colitis, against colitis-associated cancer using animal models. We therefore investigated the possible inhibition by peroxisome proliferator-activated receptor-γ (PPARγ) ligands and 5-ASA of colitis-associated colon carcinogenesis in a mouse model.

Experimental Design: A dextran sodium sulfate/azoxymethane–induced mouse colon cancer model was used, and the chemopreventive effects of 5-ASA and PPARγ ligands, given in the remission phase of colitis, against colitis-related colon carcinogenesis, were evaluated.

Results: The number of neoplasms in the mice treated with 5-ASA was significantly lower than that in the control mice. In addition, the size of the neoplasms in treated mice was also significantly smaller than that in the control mice. In contrast, no significant suppression in the number or size of the tumors was observed in the mice treated with PPARγ ligands. The proliferating cell nuclear antigen–labeling index in the tumor cells of the 5-ASA–treated mice was significantly smaller than that in the control, indicating that 5-ASA reduced tumor cell proliferation.

Conclusion: Our results revealed that 5-ASA given in the remission phase of colitis significantly suppressed the development of colitis-associated cancer in a mouse model, which indicates the clinical importance of adopting chemopreventive strategies even in UC patients in remission.

In recent decades, the prevalence of inflammatory bowel disease, i.e., ulcerative colitis (UC) and Crohn's disease has been increasing annually throughout the world. One possible reason is that patients with inflammatory bowel disease survive longer than before because of advances in treatments. On the other hand, the risk of colorectal cancer in these patients, so-called colitis-associated cancer, has also increased, especially in cases of UC. Colitis-associated cancer is believed to be a result of chronic inflammation. A recent meta-analysis has estimated the incidence rate of colitis-associated cancer at 7 per 1,000 person-years and 12 per 1,000 person-years in the second and third decades of UC, respectively (1). Therefore, attempts at prevention of colitis-associated cancer in this high-risk group of patients are considered to be important.

Recent clinical reports have suggested that treatment of UC patients with 5-aminosalicylic acid (5-ASA) might reduce the incidence of colitis-associated cancer (2, 3). Although these reports suggest that treatment of UC patients with 5-ASA may be useful for the prevention of colitis-associated cancer, the precise chemopreventive effects have not been elucidated yet. Therefore, it is considered important that the chemopreventive effect of 5-ASA and the mechanisms underlying the chemoprevention of colitis-associated cancer by 5-ASA have been investigated using animal models. Although 5-ASA is widely used in the treatment of UC to suppress colonic inflammation, no studies have been conducted to examine the chemoprevention by 5-ASA, given in the remission phase of colitis, against colitis-associated cancer using animal models. In addition, the pathogenesis of inflammatory bowel disease–related colitic cancer is still unclear, although various studies using animal

Authors' Affiliations: [1]Gastroenterology Division, [2]Department of Pathology, Yokohama City University Graduate School of Medicine, Yokohama, Japan, [3]Department of Pharmacology, Graduate School of Dentistry, Osaka University, Osaka, Japan, and [4]Biochemistry Division, National Cancer Center Research Institute, Tokyo, Japan

Received 5/16/07; revised 7/24/07; accepted 8/2/07.

Grant support: Program for Promotion of Fundamental Studies in Health Sciences of the National Institute of Biomedical Innovation, a Grant-in-Aid from the Ministry of Health, Labour, and Welfare of Japan (A. Nakajima), a grant (Kiban B) from the Ministry of Education, Culture, Sports, Science, and Technology, Japan (A. Nakajima), a grant from the Human Science Foundation (A. Nakajima), and a Princess Takamatsu Cancer Research Fund (A. Nakajima).

The costs of publication of this article were defrayed in part by the payment of page charges. This article must therefore be hereby marked *advertisement* in accordance with 18 U.S.C. Section 1734 solely to indicate this fact.

Note: Supplementary data for this article are available at Clinical Cancer Research Online (http://clincancerres.aacrjournals.org/).

I. Ikeda and A. Tomimoto contributed equally to this article.

Requests for reprints: Atsushi Nakajima, Gastroenterology Division, Yokohama City University Graduate School of Medicine, 3-9 Fuku-ura, Kanazawa-ku, Yokohama 236-0004, Japan. Phone: 81-45787-2640; Fax: 81-45787-8988; E-mail: nakajima-tky@umin.ac.jp.

doi:10.1158/1078-0432.CCR-07-1208

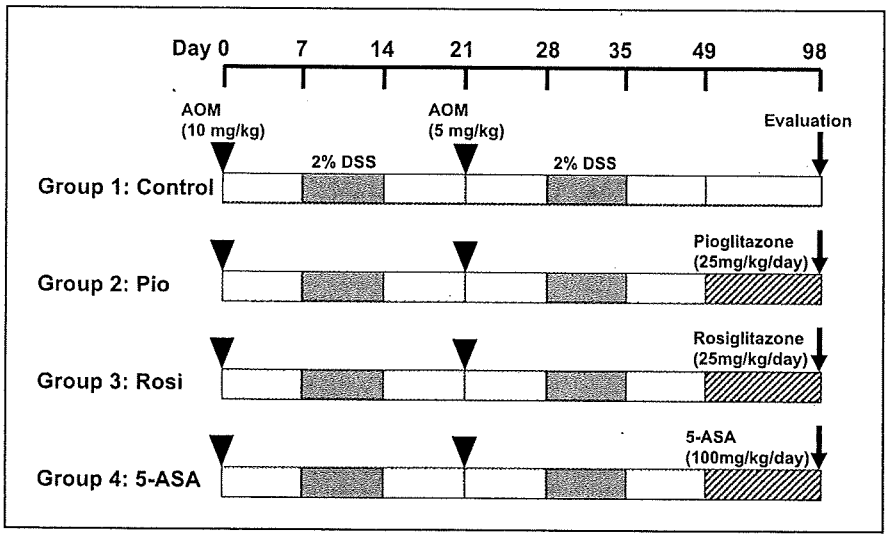

Fig. 1. Experimental protocol for investigating the chemopreventive effects of PPARγ ligands and 5-ASA in a mouse model of colitic cancer. Group 1: Control, 1 wk after the first i.p. azoxymethane (10 mg/kg) injection, the mice were given 2% DSS in drinking water for 7 d, then 1 wk after the second i.p. azoxymethane (5 mg/kg) injection, the mice were again given 2% DSS in the drinking water for 7 d. Group 2: Pio, treated with pioglitazone (25 mg/kg). Group 3: Rosi, treated with rosiglitazone (25 mg/kg). Group 4: 5-ASA, treated with 5-ASA (100 mg/kg).

models have been conducted to investigate the pathogenesis (4–6). Dextran sodium sulfate (DSS) is the most widely used chemical to induce colitis (6), and the DSS-induced colitis model is also expected to be useful for the study of inflammatory bowel disease–related colitis-associated cancer. A relationship between the severity of DSS-induced inflammation and colorectal carcinogenesis, similar to that between human UC-associated dysplasia and the cancer histopathology, has been reported (5). However, the development of these DSS-induced colitis-associated cancer models need long experimental periods or repeated administration of DSS (5). In contrast, several groups have reported that exposure of mice to a single dose of azoxymethane followed by 1 week's treatment with 2% DSS could induce colonic epithelial malignancy after 6 to 20 weeks. Therefore, the azoxymethane/DSS experimental animal models are useful models for the investigation of carcinogenesis in human UC patients.

Previously, our group reported that peroxisome proliferator–activated receptor γ (PPARγ) ligands reduced colorectal tumor formation in a mouse model of colon carcinogenesis (7). PPARγ, a nuclear hormone receptor, serves as a strong link between lipid metabolism and the regulation of gene transcription (8). PPARγ is known to regulate growth arrest and terminal differentiation of adipocytes (9). In addition, PPARγis expressed in various organs, including adipose tissue, breast epithelium, small intestine, lungs, and colon (10), and is also up-regulated in various types of cancer cells. Therefore, we conducted this study to investigate whether PPARγ ligands and 5-ASA might inhibit colitis-associated colon carcinogenesis using the DSS/azoxymethane–induced mouse colon cancer model: we evaluated the chemopreventive effects on colitis-related colon carcinogenesis in the remission stage after the induction of colitis, although in many previous studies, the drugs were given before the induction of colitis.

Materials and Methods

Chemicals and animals. All mice were treated humanely in accordance with the NIH and AERI-BBRI Animal Care and Use Committee guidelines. All animal experiments were approved by the Institutional Animal Care and Use Committee of Yokohama City University School of Medicine. Five-week-old Crj:CD-1 (ICR-1) male mice were purchased from Charles River Japan, Inc. Azoxymethane was purchased from Sigma. DSS with a molecular weight of 40,000 was purchased from MP Biomedicals. The two different PPARγ ligands, pioglitazone and rosiglitazone, were kindly provided by Takeda Chemical Industries, Ltd. (Tokyo, Japan) and GlaxoSmithKline (BN, United Kingdom), respectively. 5-ASA was kindly provided by Nisshin Kyorin Pharmaceutical Co., Ltd. (Tokyo, Japan). The dose levels of the PPARγ ligands were determined on the basis of the results of our previous studies (7).

Induction of colitis-associated cancer in the mouse model. Male ICR-1 mice were given a first i.p. injection of azoxymethane (10 mg/kg) on day 0 (see Fig. 1). Seven days after the azoxymethane injection, the mice were given 2% DSS in the drinking water for 7 days. One week after the discontinuation of DSS administration, the mice were given a second i.p. injection of azoxymethane (5 mg/kg). Then, 7 days after the second azoxymethane injection, the mice were again given 2% DSS in the drinking water for 7 days. Two weeks later, the mice were randomly divided into four groups: group 1 was fed a diet without PPARγligands or 5-ASA; groups 2 to 4 were fed diets with the PPARγligands pioglitazone (25 mg/kg, group 2) or rosiglitazone (25 mg/kg, group 3), or 5-ASA (100 mg/kg, group 4) for 49 days until sacrifice. All mice were sacrificed at the end of the study (day 98; Fig. 1).

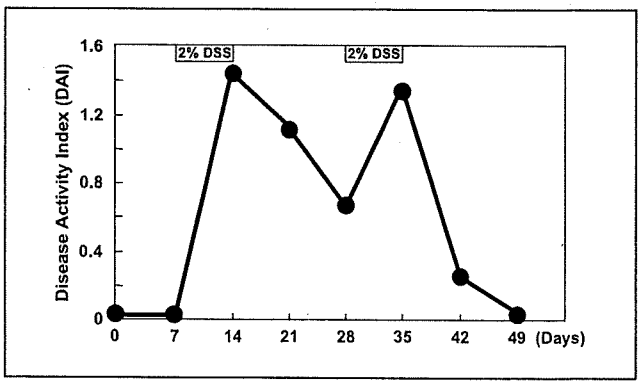

Fig. 2. The disease activity index (*DAI*) was estimated according to the method described. The disease activity increased dramatically immediately after the DSS treatment, to decrease again by 1 wk after the second treatment with DSS.

Table 1. Number and size of tumors

Group	*n*	Body weight (g)	No. of tumors	No. of tumors/mouse	Size of tumors (mm)
(1) Control	8	39.0 ± 1.3*	70	8.5 ± 4.0*	3.3 ± 1.5*
(2) Pioglitazone	6	40.8 ± 1.0*	57	9.5 ± 4.0*	3.6 ± 2.1*
(3) Rosiglitazone	6	39.5 ± 2.4*	58	8.8 ± 4.9*	3.8 ± 1.8*
(4) 5-ASA	8	40.0 ± 4.7*	38	4.0 ± 2.8*	2.4 ± 1.1*

NOTE: A total of 33 male ICR-1 mice were divided into control and experimental groups. The body weights of the mice did not change significantly. As clearly shown, 5-ASA suppressed the formation of neoplasms ($P < 0.05$). The size of the neoplasms in the colon of mice fed the diet containing 5-ASA was smaller than that in the colon specimens from other groups ($P < 0.01$).
*Mean ± SD.

Assessment of colitis. Body weight, the presence of blood in the feces, and stool consistency were recorded daily for each animal. These variables were used to calculate the average daily disease activity index for each animal, as previously described (11). The disease activity index has been shown to be well-correlated with the colon tissue damage score.

Histopathologic analysis. The histopathologic alterations in the colon were examined on H&E-stained sections. A pathologist (Y. Nagashima) diagnosed the colonic neoplasms according to a previously described method (12).

Immunohistochemistry. Immunohistochemistry for proliferating cell nuclear antigen (PCNA) and β-catenin was done. For PCNA immunohistochemistry, we used a PCNA staining kit (ZYMED Laboratories) in accordance with the manufacturer's instructions. For β-catenin immunohistochemical analysis, we used a monoclonal antibody directed against β-catenin (1:1,200 dilution; BD Transduction Laboratories) and a Vectastain ABC kit (Vector Laboratories).

The PCNA labeling index was expressed as the percentage of cells showing positive staining for PCNA relative to the total number of cells. At least five representative areas in a section were selected by light microscope examination at 400-fold magnification and a minimum of 3,000 tumor cells were counted (13).

Statistical analysis. Statistical analysis of the changes in the body weights of the mice, number of neoplasms, and size of neoplasms were done using a χ^2 test. Differences were considered significant when at $P < 0.05$.

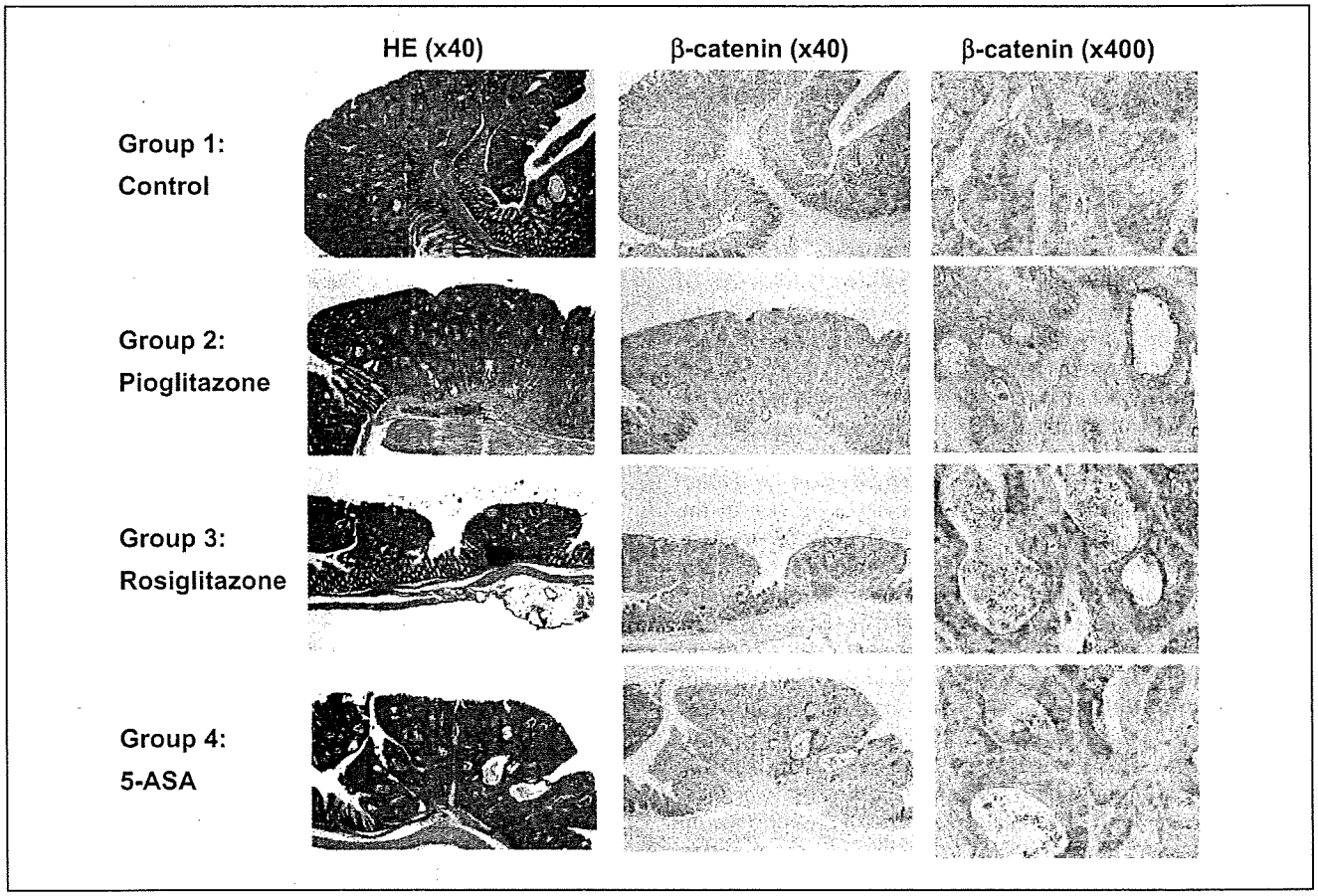

Fig. 3. Microscopic examination of H&E-stained colon sections and β-catenin staining of the tumors. Left, H&E staining (original magnification, ×40). Middle, β-catenin staining (original magnification, ×40). Right, β-catenin staining (original magnification, ×400).

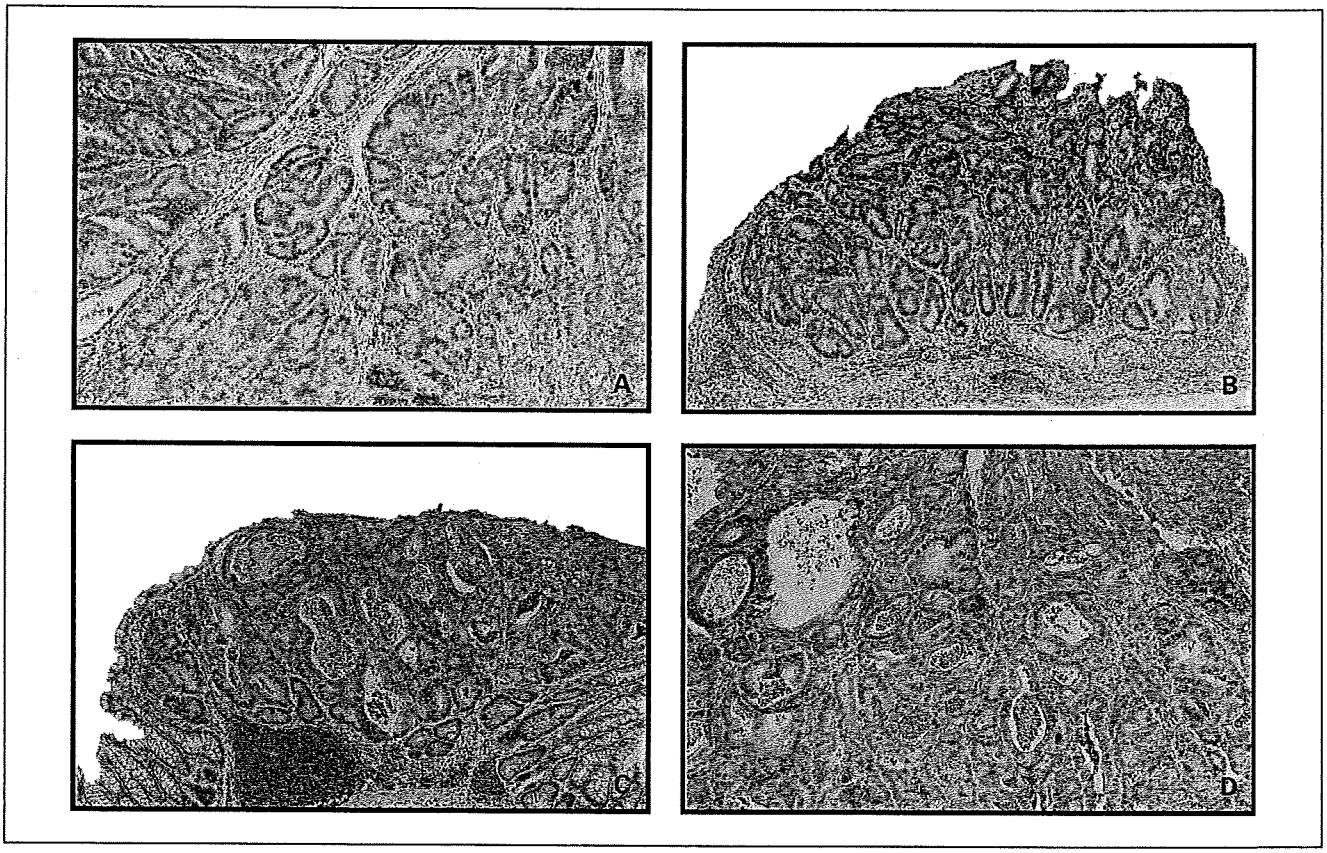

Fig. 4. Immunohistochemistry of PCNA in the tumor cells. *A*, control; *B*, pioglitazone treatment; *C*, rosiglitazone treatment; and *D*, 5-ASA treatment, respectively (original magnification, ×100).

Results

Disease activity index and body weight changes. The disease activity index was estimated according to the method described previously (11). The disease activity increased dramatically immediately after DSS treatment, to decrease again by 1 week after the second treatment with DSS (Fig. 2). The body weights of the mice measured at the end of the study period are shown in Table 1. No significant changes in the mean body weights of the mice was observed in any of the groups.

5-ASA, but not the PPARγ ligands, suppressed tumor formation in the azoxymethane/DSS mice. The number and size of the tumors in the colon specimens obtained from the mice of each group at the end of the study period are shown in Table 1. The number of neoplasms in the colon specimens from the mice treated with 5-ASA (group 4) was significantly lower than that in the colon of the control animals (group 1, $P < 0.05$). In addition, the size of the neoplasms in the colon specimens of the mice treated with 5-ASA were significantly smaller than that in the colon of the control mice. In contrast, no significant decrease of the tumor number and size was observed in the colon specimens from the mice treated with the PPARγ ligands.

Pathologic findings. H&E-stained sections of the tumors from all the groups are shown in Fig. 3. Macroscopically, nodular, polypoid tumors were observed in the middle and distal colon in all the groups. No differences in the morphologic characteristics of the tumors were observed among the groups.

Immunohistochemistry for PCNA and β-catenin. The PCNA labeling index (normal epithelial cells and tumor cells) values are shown in Table 2. The PCNA labeling index in the epithelial cells did not differ significantly among the groups ($P > 0.05$; Supplementary Figure). However, the PCNA labeling index in

Table 2. PCNA labeling index in the colon epithelial cells and tumor cells

Group no., treatment	PCNA-labeling index	
	Non-tumor cells (%)	Tumor cells (%)
(1) Control	26.10 ± 5.31*	45.29 ± 8.02*
(2) Pioglitazone	20.94 ± 8.08*	41.32 ± 8.21*
(3) Rosiglitazone	18.25 ± 2.40*	48.20 ± 11.26*
(4) 5-ASA	23.04 ± 6.34*	30.60 ± 6.61*

NOTE: The PCNA labeling index is expressed as the percentage of cells showing positive staining for PCNA relative to the total number of cells examined. At least five representative areas in a section were selected by light-microscopic examination at 400-fold magnification and a minimum of 3,000 tumor cells were counted. No significant differences in the PCNA labeling index of non-tumor cells was observed among the groups ($P > 0.05$). 5-ASA significantly decreased the PCNA labeling index in the tumor cells ($P < 0.05$).
*Mean ± SD.

the tumor cells in group 4 (5-ASA treatment), but not groups 2 or 3 (treated with the PPARγ ligands), was significantly smaller than that in group 1 (control, $P < 0.05$). Typical microscopic photographs are shown in Fig. 4. Strong β-catenin expression was seen in the nucleus and cytoplasm of the tumor cells, but there were no significant differences among the tumors in the four groups (Fig. 3, *middle* and *right*).

Discussion

In the present study, we clearly showed the chemopreventive effect of 5-ASA against colitis-associated cancer in the remission stage. In contrast, the PPARγ ligands showed no suppressive effect against neoplasm formation. Previously, our group and others have reported that the PPARγ ligands effectively inhibited the colonic inflammation associated with DSS administration, trinitrobenzene sulfonic acid–induced colitis, as well as aberrant crypt foci formation in many animal models (5, 14, 15). However, most of these reports examined the preventive effect of PPARγ ligand therapy, i.e., the PPARγ ligands were given before the induction of inflammation (pretreatment). In the present study, we gave the PPARγ ligands and 5-ASA 2 weeks after the end of DSS treatment. Therefore, all mice were in the remission stage after the induction of colitis. The remission stage was also confirmed by the disease activity index, as shown in Fig. 2 and in the Supplementary Table. As PPARγ ligands have antiinflammatory actions, their antitumor effects against colitis-associated cancer shown in previous studies might be the result of their antiinflammatory effects in colitis-associated cancer (16). This might also be the reason why the PPARγ ligands showed no suppressive effect against tumor development in our present study.

In the present study, 5-ASA markedly suppressed the development of colitic cancer. Although the PCNA labeling index in the non–tumor colonic epithelium did not differ significantly among the groups, only 5-ASA alone significantly suppressed the PCNA labeling index in the tumor cells. These results suggest that 5-ASA may reduce tumor cell but not normal epithelial cell proliferation. Further investigations will be required to clarify the detailed mechanisms.

In conclusion, we found that only 5-ASA given in the remission stage of colitis significantly suppressed the development of colitis-associated cancer in a mouse model. Our results showed the clinical importance of adopting a chemopreventive strategy in UC patients in remission.

References

1. Eaden JA, Abrams KR, Mayberry JF. The risk of colorectal cancer in ulcerative colitis: a meta-analysis. Gut 2001;48:526–35.
2. Bernstein CN, Eaden J, Steinhart AH, Munkholm P, Gordon PH. Cancer prevention in inflammatory bowel disease and the chemoprophylactic potential of 5-aminosalicylic acid. Inflamm Bowel Dis 2002;8:356–61.
3. Rubon DT, Lashner BA. Will a 5-ASA a day keep the cancer (and dysplasia) away? Am J Gastroenterol 2005;100:1345–53.
4. Seril DN, Liao J, Yang CS. Oxidative stress and ulcerative colitis-associated carcinogenesis: studies in humans and animal models. Carcinogenesis 2003;24:353–62.
5. Cooper HS, Murthy S, Kido K, Yoshitake H, Flanigan A. Dysplasia and cancer in the dextran sulfate sodium mouse colitis model. Relevance to colitis-associated neoplasia in the human: a study of histopathology, β-catenin and p53 expression and the role of inflammation. Carcinogenesis 2000;21:757–68.
6. Suzuki R, Kohno H, Sugie S, Tanaka T. Sequential observations on the occurrence of preneoplastic and neoplastic lesions in mouse colon treated with azoxymethane and dextran sodium sulfate. Cancer Sci 2004;95:721–7.
7. Osawa E, Nakajima A, Wada K, et al. Peroxisome proliferator-activated receptor-γ ligands suppress colon carcinogenesis induced by azoxymethane in mice. Gastroenterology 2003;124:361–7.
8. Forman BM, Tontonoz P, Chen J, Brun RP, Spiegelman BM, Evans RM. 15-Deoxy-δ 12,14-prostaglandin J2 is a ligand for the adipocyte determination factor PPAR γ. Cell 1995;83:803–12.
9. Kubota N, Terauchi Y, Miki H, et al. PPAR γ mediates high-fat diet-induced adipocyte hypertrophy and insulin resistance. Mol Cell 1999;4:597–609.
10. Lefebvre AM, Auwerx J. PPARγ is induced during differentiation of colon epithelium cells. J Endocrinol 1999;162:331–40.
11. Cooper HS, Murthy SN, Shah RS, Sedergran DJ. Clinicopathologic study of dextran sulfate sodium experimental murine colitis. Lab Invest 1993;69:238–49.
12. Ward JM. Morphogenesis of chemically induced neoplasms of the colon and small intestine in rats. Lab Invest 1974;30:505–13.
13. Watanabe I, Toyoda M, Okuda J, et al. Detection of apoptotic cells in human colorectal cancer by two different *in situ* methods: antibody against single-stranded DNA and terminal deoxynucleotidyl transferase-mediated dUTP-biotin nick end-labeling (TUNEL) methods. Jpn J Cancer Res 1999;90:188–93.
14. Tanaka T, Kohno H, Yoshitani S, et al. Ligands for peroxisome proliferators-activated receptors α and γ inhibit chemically induced colitis and formation of aberrant crypt foci in rats. Cancer Res 2001;61:2424–8.
15. Su CG, Wen X, Bailey ST, et al. A novel therapy for colitis utilizing PPAR-γ ligands to inhibit the epithelial inflammatory response. J Clin Invest 1999;104:383–9.
16. Kohno H, Suzuki R, Sugie S, Tanaka T. Suppression of colitis-related mouse colon carcinogenesis by a cox-2 inhibitor and PPAR ligands. BMC Cancer 2005;5:46.

Tumor-suppressive *miR-34a* induces senescence-like growth arrest through modulation of the E2F pathway in human colon cancer cells

Hiroshi Tazawa, Naoto Tsuchiya, Masashi Izumiya, and Hitoshi Nakagama*

Biochemistry Division, National Cancer Center Research Institute, 5-1-1 Tsukiji, Chuo-ku, Tokyo 104-0045, Japan

Communicated by Takashi Sugimura, National Cancer Center, Tokyo, Japan, August 4, 2007 (received for review June 6, 2007)

Accumulating evidence suggests a role for microRNAs in human carcinogenesis as novel types of tumor suppressors or oncogenes. However, their precise biological role remains largely elusive. In the present study, we aimed to identify microRNA species involved in the regulation of cell proliferation. Using quantitative RT-PCR analysis, we demonstrated that *miR-34a* was highly up-regulated in a human colon cancer cell line, HCT 116, treated with a DNA-damaging agent, adriamycin. Transient introduction of *miR-34a* into two human colon cancer cell lines, HCT 116 and RKO, caused complete suppression of cell proliferation and induced senescence-like phenotypes. Moreover, *miR-34a* also suppressed *in vivo* growth of HCT 116 and RKO cells in tumors in mice when complexed and administered with atelocollagen for drug delivery. Gene-expression microarray and immunoblot analyses revealed down-regulation of the E2F pathway by *miR-34a* introduction. Up-regulation of the p53 pathway was also observed. Furthermore, 9 of 25 human colon cancers (36%) showed decreased expression of *miR-34a* compared with counterpart normal tissues. Our results provide evidence that *miR-34a* functions as a potent suppressor of cell proliferation through modulation of the E2F signaling pathway. Abrogation of *miR-34a* function could contribute to aberrant cell proliferation, leading to colon cancer development.

microRNA | p53 | adriamycin | atelocollagen

Development of human tumors is associated with genetic and/or epigenetic alterations, which result in abnormal gene-expression profiles (1–3). Genetic alterations, such as gene amplifications, deletions, chromosomal translocations, and point mutations, induced in cells result in activation or inactivation of oncogenes and tumor suppressor genes (1), whereas epigenetic changes are defined by hyper- or hypomethylation of CpG sites in promoter regions and modifications of histones (2, 3). In addition, another class of perturbation has recently attracted attention in relation to cancer development; namely, posttranscriptional regulation of gene expression by noncoding RNA, including microRNA (miRNA), short interference RNA, and repeat-associated short interference RNA (4).

miRNA consists of ≈22 nucleotides and regulates gene expression in a posttranscriptional manner by pairing with complementary nucleotide sequences in 3′ untranslated regions (UTRs) of target mRNAs (5). Precise chronological and topological regulation of posttranscriptional gene silencing by miRNA is essential for animal development and tissue differentiation (6), and abnormal expression is suggested to be associated with various human disorders, including cancer (7–9). Recently, mutations of *miR-16-1* and *miR-15a* genes have been reported in chronic lymphocytic leukemia patients (10), and the available results suggest a crucial involvement of aberrant miRNA expression in human carcinogenesis. However, the precise, critical roles of individual miRNAs largely remain to be elucidated.

We recently identified SND1/Tudor-SN as a C-rich DNA/RNA-binding protein (11), and Caudy *et al.* (12) reported it to be a component of RNA-induced silencing complex (RISC). We also demonstrated its frequent up-regulation in human colon cancers (13). Furthermore, it was also overexpressed in precancerous lesions induced by chemical carcinogens in rats (13). Although the detailed molecular mechanisms underlying the induction of SND1 in colon epithelial cells are not yet clear, alteration of its expression could be accompanied by the changes in the expression of miRNA species caused by some environmental insults. Therefore, we hypothesize that expression of a subset of miRNA species and components of miRNA effector complexes, including SND1, is affected by cytotoxic stresses and could play an important role in the onset and progression of colon carcinogenesis.

Recently, aberrant up- and down-regulation of miRNA species in human colon cancers has been reported (7–9). However, which miRNA species are actually implicated in human colon cancer development remains to be elucidated. Therefore, we have attempted to isolate miRNA species associated with cell proliferation control in colon epithelial cells. Aiming to this goal, we here used human colon cancer HCT 116 cells harboring wild-type p53 to identify miRNA species induced after cell proliferation arrest when treated with a low concentration of ADR. By comparing the miRNA responses after ADR treatment between HCT 116 and HCT 116 p53 knockout (HCT 116 $p53^{-/-}$) cell lines (14), we identified the *miR-34* family as an ADR-responsive miRNA group in a p53-dependent manner. Focusing on *miR-34a* that showed relatively high-expression levels among the *miR-34* family members in HCT 116 cells, we further investigated the biological effects of *miR-34a* on cell proliferation both *in vitro* and *in vivo* settings. Expression levels of *miR-34a* in human colon cancers were also determined, and their possible role in human colon cancer development is discussed below.

Results

Induction of the *miR-34* Family in Response to ADR in Human Colon Cancer HCT 116 Cells. Among 157 miRNAs assembled in the list of the TaqMan MicroRNA Assays Human Panel, seven miRNAs (*miR-16*, *-34a*, *-34b*, *-34c*, *-146*, *-147*, and *-205*) were increased 2-fold or greater in ADR-treated (100 ng/ml, 16 h) HCT 116 cells as compared with nontreated cells in the first experiment [supporting information (SI) Table 1]. In two other independent experiments, we analyzed the expression of these seven miRNAs as described above along with 17 other miRNAs that had shown

Author contributions: H.T., N.T, and H.N. designed research; H.T., N.T., and M.I. performed research; H.T., N.T., M.I., and H.N. analyzed data; and H.T., N.T., and H.N wrote the paper.

The authors declare no conflict of interest.

Abbreviations: miRNA, microRNA; ADR, adriamycin; SA-β-gal, senescence-associated β-galactosidase.

*To whom correspondence should be addressed. E-mail: hnakagam@gan2.res.ncc.go.jp.

This article contains supporting information online at www.pnas.org/cgi/content/full/0707351104/DC1.

www.pnas.org/cgi/doi/10.1073/pnas.0707351104

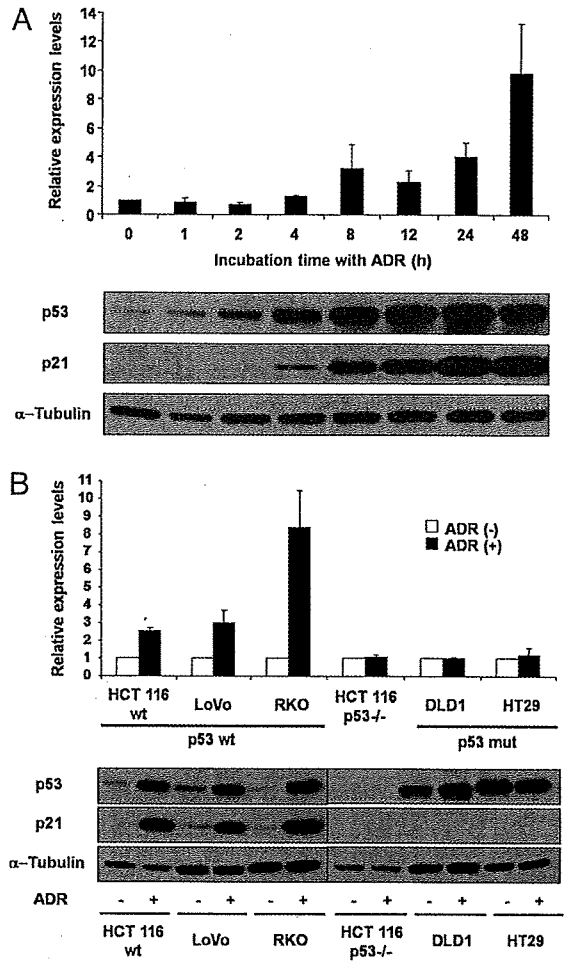

Fig. 1. Induction of *miR-34a* expression after treatment with ADR in colon cancer cell lines with wild-type p53. (*A*) HCT 116 cells were incubated in the presence of ADR at a concentration of 100 ng/ml, and *miR-34a* expression was analyzed at the indicated time points by using quantitative real-time RT-PCR. The value for *miR-34a* at time 0 was set at 1, and the relative amounts of *miR-34a* at the other time points were plotted as fold induction. Immunoblots under the graph indicate the accumulation of p53 and p21 at each time point. α-Tubulin was used as a loading control. (*B*) Induction of *miR-34a* in p53 wild-type and p53-knockout or -mutated colon cancer cell lines after 16 h incubation in the culture medium with or without ADR. The relative amounts of *miR-34a* in ADR-treated cells were calculated as described above. Open and filled bars represent nontreated and ADR-treated cells, respectively. Immunoblots under the graph indicate the accumulation of p53 and p21 detected in the six colon cancer cell lines.

no change after ADR treatment in the first experiment. The *miR-34* family, *miR-34a*, *-34b*, and *-34c*, were reproducibly induced >2-fold after ADR treatment, whereas four other miRNAs (*miR-16*, *-146*, *-147*, and *-205*) were not induced consistently (SI Table 1). The expression of 17 miRNAs, representing the miRNA not being responsive to ADR in HCT 116 cells, did not change compared with the nontreated cells. For further analysis, we focused on *miR-34a* because substantial expression of *miR-34a* was observed, although, in contrast, expression levels of the other *miR-34* family members, *miR-34b* and *-34c*, were very low.

***miR-34a* Induction Depends on p53 Activation.** *miR-34a* expression was increased in a time-dependent manner after ADR treatment, rising 3.2-fold at 8 h and >10-fold at 48 h (Fig. 1*A*). We also observed that p53 and p21 started to accumulate at 2 and 4 h, respectively, and the accumulation continued until 48 h after treatment (Fig. 1*A*). HCT 116 $p53^{-/-}$ cells showed no change in expression of *miR-34a* after ADR treatment (Fig. 1*B*). To confirm that the induction of *miR-34a* depends on p53, other human colon cancer cell lines, either with wild-type *p53* genes (LoVo and RKO) or mutated *p53* genes (DLD1 and HT29), were analyzed (Fig. 1*B*). As expected, LoVo and RKO cells exhibited increased expression of *miR-34a* similar to HCT 116 cells, but DLD1 and HT29 cells showed no change, like the HCT 116 $p53^{-/-}$ cells. Accumulation of p53 and p21 was observed in HCT 116, LoVo, and RKO cells, whereas HCT 116 $p53^{-/-}$ cells showed no accumulation, and DLD1 and HT29 cells expressing mutant p53 showed consistent levels of p53 and no accumulation of p21. These results indicate that *miR-34a* is induced in a p53-dependent manner after ADR treatment.

***miR-34a* Inhibits Cell Proliferation of HCT 116 and RKO Cells.** The marked induction of *miR-34a* after p53 activation, prompted us to investigate whether *miR-34a* functions as a tumor suppressor. The introduction of *miR-34a* caused a remarkable inhibition of cell proliferation in both HCT 116 and RKO cells compared with that of control miRNA (Fig. 2*A*). Immunoblot analysis for apoptosis-specific markers, PARP and caspase-3, revealed no significant induction of apoptosis-related cellular responses in either cell line by *miR-34a* (Fig. 2*B*), indicating that the inhibitory effect of *miR-34a* on cell proliferation is not mainly caused by apoptotic response.

***miR-34a* Down-Regulates the E2F Signaling Pathway and Up-Regulates the p53 Signaling Pathway.** Comprehensive gene-expression analysis using an Agilent (Agilent Technologies, Santa Clara, CA) microarray platform revealed 287 genes to be down-regulated and 326 genes to be up-regulated 2-fold or greater in both HCT 116 and RKO cells transfected with *miR-34a*, compared with those transfected with control miRNA (SI Tables 2–4). As for the down-regulated genes, *E2F1*, *E2F2*, and some E2F-target genes, including *DHFR*, *MCM3*, and *MCM10*, were observed among the list. Genes associated with cell-cycle progression, *CDK4* and *CDC25C*, were also down-regulated. Among the up-regulated genes, a subset of p53-target genes, including *CDKN1A* (p21), *TP53INP1*, *ATF3*, *IKIP*, *ICAM1*, and *PTPRE*, was apparent. Based on these observations, we hypothesized that E2F-family proteins could be candidate targets for *miR-34a*.

We then examined the protein levels of E2F-family proteins, E2F-1, -2, and -3, in HCT 116 and RKO cells. E2F-3 is a predicted target for *miR-34a* in the databases (PicTar web site, http://pictar.bio.nyu.edu), but no further information on E2F-3 with regard to its biological relationship with *miR-34a* is available. As shown in Fig. 2*C*, introduction of *miR-34a* decreased the accumulation of E2F-1 and -3. E2F-2 was not detectable in either case (data not shown). Accumulation of the p53 and p21 proteins was also observed by introduction of *miR-34a* in both cell lines, reflecting the results of global gene-expression analysis by microarray system. These observations indicate that introduction of *miR-34a* causes the down-regulation of the E2F pathway, leading to the up-regulation of the p53/p21 pathway. A possible mechanism for the up-regulation of p53 and its downstream target is discussed below.

***miR-34a* Induces Senescence-Like Phenotypes.** We observed that introduction of *miR-34a* in HCT 116 cells caused senescence-like phenotypes with positive staining for senescence-associated β-galactosidase (SA-β-gal) and enlarged cellular size (Fig. 2*D*). RKO cells also showed similar morphological changes with enlarged cellular size by *miR-34a* introduction, although few SA-β-gal-positive cells were observed (Fig. 2*D*). We also ob-